CONSTANS-FKBP12 interaction contributes to modulate photoperiodic flowering in *Arabidopsis*

Gloria Serrano-Bueno[1*], Fatima E. Said[1*], Pedro de los Reyes[1], Eva I. Lucas-Reina[1†], M. Isabel Ortiz-Marchena[1], José M. Romero[1,2] and Federico Valverde[1]

[1] Instituto de Bioquímica Vegetal y Fotosíntesis, CSIC-Universidad de Sevilla, 49 Americo Vespucio, 41092 Sevilla, Spain; [2] Departamento de Bioquímica Vegetal y Biología Molecular, Facultad de Biología, Universidad de Sevilla, Reina Mercedes, 41012 Sevilla, Spain.

Author for correspondence:
Federico Valverde
Tel. +34 954489525
Email: federico.valverde@ibvf.csic.es
* These authors contributed equally to this work.

[†] Present address: Instituto de Hortofruticultura Subtropical y Mediterránea-Universidad de Málaga-CSIC, Departamento de Biología Molecular y Bioquímica, Facultad de Ciencias-Universidad de Málaga, 29071 Málaga, Spain.

Total word count: 8,827.

Running head: Role of FKBP12 in CONSTANS activity modulation

Key words: Floral transition, photoperiodic flowering, CONSTANS, FKBP12, posttranslational modification, protein stability.

SUMMARY

Flowering time is a key process in plant development. Photoperiodic signals play a crucial role in the floral transition in *Arabidopsis thaliana* and CONSTANS (CO) protein has a central regulatory function that is tightly regulated at the transcriptional and post-translational levels. CO protein stability depends on a light-driven proteasome process that optimizes its accumulation in the evening to promote the production of the florigen FLOWERING LOCUS T (FT) and induce seasonal flowering. To further investigate the posttranslational regulation of CO protein we have dissected its interactome network employing *in vivo* and *in vitro* assays and molecular genetics approaches. The immunophilin FKBP12 has been identified as a CO interactor in *Arabidopsis* that regulates its accumulation and activity. FKBP12-CO interact through the CCT domain, affecting CO stability and function. *fkbp12* insertion mutants show a delay in flowering time, while *FKBP12* overexpression accelerates flowering, and these phenotypes can be directly related to a change in FT protein accumulation. The interaction is conserved between the *Chlamydomonas* algal orthologues CrCO-CrFKBP12, revealing an ancient regulatory step in photoperiod regulation of plant development.

INTRODUCTION

The precise timing of the floral transition is a key decision for a plant, as it is directly related to the success of its offspring (Austen *et al.*, 2017). The floral transition is influenced by internal and external cues that determine the correct time of the year to flower (Levin, 2009). In recent literature, an intricate network of genes involved in the floral transition in the model plant *Arabidopsis thaliana* has been unveiled (Pajoro *et al.*, 2014). The vernalization (Song *et al.*, 2012), photoperiodic and internal (Andrés & Coupland, 2012) pathways define well-delimited, but still interconnected pathways that control the floral transition in *Arabidopsis* (Blümel *et al.*, 2015).

The photoperiod pathway involves the response of the plant to the length of the day and the way they will flower in response to changes in light-driven circadian rhythms (Shim *et al.*, 2017). Thus, *A. thaliana* is a facultative long-day (LD) plant that will flower earlier under a 16 h light: 8 h dark day than in a short day (SD) of 8 h light: 16 h dark. However, other plants, such as rice, will respond differently by flowering when daylight recedes, or even will not respond to day length, as some wild tomato species (Jackson, 2008). The gene *CONSTANS* (*CO*) plays a pivotal role as CO protein binds in a complex to the promoter of the florigenic gene *FLOWERING LOCUS T* (*FT*) (Wenkel *et al.*, 2006; Tiwari *et al.*, 2010; Gnesutta *et al.*, 2017) inducing its expression under LD conditions in the phloem companion cells (An *et al.*, 2004). Then, FT protein will move through the phloem to the shoot apical meristem (SAM) to induce the activation of the flower developmental program (Mathieu *et al.*, 2007).

CO will also activate the expression of several genes involved in the transmission of this flowering signal such as the starch synthase *GBSS*, that promotes a temporal increase in the concentration of soluble sugars during the floral transition (Ortiz-Marchena *et al.*, 2014) or proline synthesis (Mattioli *et al.*, 2009). Thus, the photoperiod pathway also controls signals, such as an increase in mobile sugars from starch (Ortiz-Marchena *et al.*, 2015) that would systemically coordinate this transition.

Most of the information accumulated around flowering time control takes place at the transcriptional level (Guo *et al.*, 2017) but important posttranslational steps are also pivotal to this process (Swiezewski *et al.*, 2009; Posé *et al.*, 2013). CO protein is

particularly sensitive to posttranslational modifications as both phosphorylation (Sarid-Krebs *et al.*, 2015) and ubiquitination (Valverde *et al.*, 2004) play an important role in its stability. In these signaling processes the RING finger E3 ubiquitin ligases CONSTITUTIVE PHOTOMORPHOGENIC 1 (COP1) and HIGH EXPRESSION OF OSMOTICALLY RESPONSIVE GENE 1 (HOS1) act in a stepwise manner to control the nocturnal (COP1) and early morning (HOS1) proteasome-mediated degradation of CO, limiting its presence to LD evenings (Jang et al, 2008; Lazaro *et al.*, 2012). Also, blue light through Cryptochrome 2 (CRY2), affecting COP1 (Valverde et al, 2004), and red light through Phytochrome B (PHYB), affecting HOS1 (Lazaro *et al.*, 2015), are important in the process.

The small immunophilin FKBP12 (FK506 Binding Protein 12 kD) has been thoroughly characterized in animals as an immunorepressor due to its capacity to bind and inhibit the phosphatase calcineurin through the drug K506 (tacrolimus) (Kang *et al.*, 2008). FKBP12 can also bind TOR (Target Of Rapamycin) kinase by forming a covalent bond rapamycin-FKBP12-TOR that inactivates this essential kinase (Loewith *et al.*, 2002). Although algae, such as *Chlamydomonas*, are sensitive to rapamycin (Crespo *et al.*, 2005), higher plants are mostly insensitive to the drug because plant FKBP12 lacks the key amino acid residues that mediate the interaction with TOR (Menand *et al.*, 2002). This has been proposed to be an evolutionary acquisition of spermatophytes in response to the long cohabitation with rapamycin-producing bacteria in soil (Xiong *&* Sheen, 2012). *Arabidopsis* FKBP12 has the prolyl isomerase activity that characterizes all FKBPs family members, which are able to alter the state of proline residues within a polypeptide chain from cis to trans forms (Gollan *et al.*, 2012), thus having a crucial role in protein structure. FKBPs have also been involved in supramolecular complexes that help partners modify its structure, identify substrates and move through cellular compartments (Kim *&* Chen, 2000). Although some *fkbps* mutants display a strong developmental phenotype, plant *fkbp12* mutants have not been described in detail and no phenotypic description of its mutation or developmental defects has been defined. In fact, only a single partner of FKBP12, (FKBP12 INTERACTING PROTEIN 37) AtFIP37 (Faure *et al.*, 1998) has been identified in plants, and a role in trichome endoreduplication proposed (Vespa *et al.*, 2004).

In this work, we describe an alternative role for FKBP12 in the posttranslational modification of CO in *Arabidopsis*. The interaction with FKBP12 influences CO stability and promotes its activity. Therefore, not only CO activity is compromised by the action of photoreceptors, ubiquitin ligases and protein kinases but also through the interaction with the small chaperone-like FKBP12. CO-FKBP12 interaction involves the same domain that mediates COP1 and HOS1 interaction and, therefore, could also interfere in CO stability. Both mutant and overexpression lines show a slight but consistent floral phenotype that can be traced to small changes in *FT*, but not *CO*, expression patterns. The interaction is conserved between the *C. reinhardtii* homologous proteins CrCO (Serrano *et al.*, 2009) and CrFKBP12 (Crespo *et al.*, 2005) providing a clue to the evolutionary importance of the complex. Therefore, this work unveils a different role for CO activity modification at the posttranslational level that could be important to understand and modify flowering time in other plant species like crops.

RESULTS

Identification of FKBP12 as a CONSTANS-interacting protein

In order to identify other binding partners involved in CONSTANS posttranslational regulation, the yeast-based Split-Ubiquitin-System (SUS) approach was used (Johnsson & Varshavsky, 1999; Pusch *et al.*, 2012). As CO can self-activate transcription in traditional Y2H screenings (Ben-Naim *et al.*, 2006), an assay exclusively based on protein interactions was chosen. A library constructed from 4-weeks-old plants grown in LD and harvested during daylight (I. Ottenschläger and F. Santos, K. Palme laboratory) was screened. In this SUS version, prey vector includes *Arabidopsis* cDNA library clones fused to the N-terminal part of ubiquitin attached to *URA3* gene. *URA3* codes for the enzyme R-URA, which catalyses the synthesis of the toxin 5-fluorouracil from the protoxin 5-FOA (5-Fluoroorotic acid). In Bait vector, CO ORF is fused to ubiquitin C-terminal part. Reconstitution of ubiquitin, meaning interaction between prey and bait, degrades the R-URA protein by the proteasome, allowing the growth of colonies in the presence of 5-FOA and the selection of clones expressing the interacting proteins (Dünnwald *et al.*, 1999). This allowed to use the whole CO protein rather than isolated domains (Wenkel

et al., 2006) or artificial fusions (Ben-Naim *et al.*, 2006) and opened the possibility to describe different interactions.

Conducting five independent SUS experiments, more than 25,000 independent interactions were tested and 42 positive clones, representing 31 different putative CO binding partners, identified (Table 1). The putative CO interactors were grouped according to functional terms using the agriGO and TAIR tools (Figure S1a, b). Gene Ontology (GO) terms significantly enriched among these interactors were related with macromolecular interactions (DNA/RNA and proteins), transferase/hydrolase activity and stress/biotic/abiotic stimulants. Fifteen of the proteins were predicted as nuclear, but others were allocated to organelles or cytosol, reflecting the wide range of possible interactions allowed by the SUS protocol. Even considering that some of them might be artifactual, cytosolic interactors have been described as important regulators of transcription factors (TFs) before (Cyert, 2001; Igarashi *et al.*, 2001; Wilson *et al.*, 2016).

Among these interactors, clones including the small immunophilin FKBP12 (At5g64350) (Table 1, highlighted in grey) were repeatedly rescued in the SUS screening. In fact, tomato FKBP12 had been previously identified in Y2H screening as a putative interactor of a CO homologue (SlCOL1) using a tomato cDNA library (Ben-Naim *et al.*, 2006). As FKBPs are mainly cytosolic proteins and several reports had shown that they could act as chaperones involved in protein folding and cellular transport (Geisler *&* Bailly, 2007; Gollan *et al.*, 2012), they were excellent candidates for CO posttranslational regulators.

Interaction between CO and FKBP12

CO-FKBP12 interaction was confirmed by experiments in bacteria, yeast and plants. First, *CO* and *FKBP12* complete ORFs were expressed in *E. coli* under the same inducible promoter (pETDuet-1, Experimental procedures) so that upon IPTG induction both proteins were produced with a similar stoichiometry (Figure S3a). To identify the polypeptides, CO was S·tagged (S·CO) and FKBP12 His·tagged (H·FK) (Figure 1a-b and S3a). When the extracts were incubated with TALON (GE Healthcare) His-affinity resin and washed, immunoblots using αHis (Sigma Aldrich) showed that H·FK was retained in the beads (Figure 1a, lanes Ft, W) and was eluted by rising imidazole concentration

(Figure 1a, lane El). When the same blot was restriped and tested with a specific CO antibody (αCO, Experimental procedures) it showed that S·CO was effectively co-expressed with H·FK (Figure 1a, In lane), but further, the interaction was confirmed by showing that S·CO was retained (Figure 1a, lanes Ft, W) and co-eluted in the same fraction as H·FK (Figure 1a, El lane). Controls in which S·CO alone were expressed in *E coli* showed that CO presented a very low affinity to the TALON resin (Figure 1b).

To further test CO-FKBP12 interaction, a transient interaction assay in *Nicotiana benthamiana* cells, was used. CO ORF was fused at the carboxyl end to the Yellow Fluorescent Protein (CO-YFP) and FKBP12 to the cyan fluorescent protein (FK-CFP). The fluorescents constructs were transiently expressed in *Nicotiana* via *Agrobacterium* transformation (Voinnet *et al.*, 2003) and observed under the confocal microscope (Figures 1c and S2). While FK-CFP alone showed a mainly cytosolic localization in *Nicotiana* cells (Figure S2a) and CO-YFP, as expected, was nuclear (Figure S2b), surprisingly, co-expression of both constructs showed a nuclear-cytosolic signal in *Nicotiana* in both yellow and blue light when excited at their corresponding exciting light wavelengths (Figure S2c). When the same plants were excited with specific CFP exciting lights and detected at the YFP emission window, the nuclear-cytosolic signal (Figure 1c) indicated a FRET effect. This effect was quantified with an efficiency of 10-20 % higher than the control including FK-CFP and the yellow protein alone (Figure 1c, right and S2e). The FRET effect strongly supported the direct *in vivo* interaction between both proteins. A co-expression experiment was repeated in onion epidermal cells by transient assays particle bombardment, showing a clear co-localization signal (Figure S2d). The interaction in *Nicotiana* was also tested by co-immunoprecipitation experiments. In this experiment we used the same CO-YFP plants and plants FK-TAP that fused FKBP12 to the TAP tag at the carboxyl end from vector cTapi.289.gw (Rohila *et al.*, 2004). When both constructs were co-expressed in *Nicotiana* cells and protein extracts incubated with a GFP nanobody fused to magnetic beads (chromotek), the eluting solution included both CO and FKBP12 (Figure S2b, ELUTION FK-TAP/CO-YFP lane) while all other controls did not show a positive result (Figure S2b, ELUTION) using specific αCO and αFKBP12 (αFK) antibodies (experimental procedures).

In the confocal images and co-IP experiments in *Nicotiana* we had observed that YFPCO protein abundance seemed to be enhanced in the presence of TAP-tagged FKBP12, while the stability of YFP-tagged version of CO expressed alone, was drastically reduced (Figure S3b). Therefore, it was interesting to test if altering the native ratio of the proteins modified their stability, so we analyzed the presence of FKBP12 in total protein extracts from *Arabidopsis* Col-0, plants overexpressing *CO* (35S:*CO*) (Onouchi *et al.*, 2000) and T-DNA null mutant co-*10* (Sail collection) (Laubinger *et al.,* 2006) employing αFK in immunoblots (Figure 1d). While FKBP12 presence was not altered in *co-10* mutant plants compared to WT Col-0 (Figure 1d), an increase in the 12 kD immunophilin band could be detected in protein extracts from plants overexpressing *CO*. Similarly, nuclear CO presence was augmented in *Arabidopsis* plants overexpressing *FKBP12* (see below) when compared to WT Col-0 extracts at comparable levels to that of plants overexpressing *CO* (Figure 1e).

Altered levels of *FKBP12* expression promote variations in flowering time

Because of FKBP12-CO interaction, the enhanced stability of the proteins and the pivotal role of CO in the floral transition, we wondered if modifying the expression of the immunophilin would alter flowering time in *Arabidopsis*. To test this possibility, two different T-DNA insertion mutants (Col-0 background) in *FKBP12* genomic region were identified: one from Salk collection (SalK_064494) named *fk12-1*, and another from Wisconsin collection (WiscDsLox1E10) named *fk12-5*. After confirming the insertion sites of the two T-DNAs (Figure S4a-b), we obtained homozygous lines with a strong reduction in FKBP12 protein levels (Figure S4c). Both mutants showed similar late flowering phenotype (see below) and were used for further experiments.

We then compared the expression of *FKBP12* in 24 h experiments in Col-0 and *fk12-1* (Figure 2). In LD, *FKBP12* mRNA expression showed a peak 4 h after dawn (ZEITGEBER TIME 4, ZT4) and a minimum expression in the middle of the day at ZT8, slowly rising through the evening and night (Figure 2a left, grey line). In SD, the pattern lacked the peak at ZT4 and showed a maximum expression at ZT12 (Figure 2a right, grey line). The expression of *FKBP12* was also followed in plants grown for two weeks in LD and then transferred to either continuous light (LL) or continuous dark (DD) conditions

and mRNA accumulation was measured during the following 48 h (Figure S5). In LL conditions (Figure S5a) *FKBP12* expression continued its rhythmic tendency through two consecutive days in continuous light. When this pattern was analyzed with the Bioconductor R package RAIN (Rhythmicity Analysis Incorporating Nonparametric methods) a significant (0.05 p-value) periodic wave form was obtained, indicating the circadian character of the expression of the gene in LL. However, when plants were transferred to DD, *FKBP12* expression drastically decreased, and no significant (0.53 p-value) periodic pattern was observed (Figure S5b). *FKBP12* expression was significantly reduced in the mutant *fk12-1* background in LD and SD, promoting the loss of circadian regulation of the gene (Figure 2a, S5c-d, black dotted lines). The reduced gene expression caused a drastic reduction in protein levels throughout the day as shown in the immunoblots and graphics of Figure 2b. While FKBP12 protein showed an increasing accumulation during the evening in LD (Figure 2b, grey line) the protein was almost completely absent in *fk12*-1 and *fk12-5* mutants (Figures 2b, black dotted line and S4c).

To generate *FKBP12* overexpression lines, the ORF was cloned behind the 35S promoter in pEG100 vector (Early *et al.*, 2006) and transformed into *Arabidopsis* Col-0 plants by floral dipping. BASTA selection produced herbicide-resistant plants among which, three T3 independent homozygous lines were selected. *FKBP12* expression in all 35S:*FKBP12* (35S:*FK*) plants was up to seven times higher than that of WT expression during LD and SD conditions (Figure S5c-d) and this resulted in a constant and very high presence of the protein during the entire photoperiod (Figure 2b, solid black line). On the other hand, as was observed *in vitro* before (Figure 1d) the stability and presence of FKBP12 protein increased in plants overexpressing *CO* (Figure 2c), so that the amount of the immunophilin closely followed that of CO during LD in 35S:*CO* plants, hinting again to a close association between both proteins.

In order to understand the possible effect of the FKBP12 on CO function, we analyzed the 24 h expression patterns of *CO* and its primary target *FT*, in *fkbp12* mutant backgrounds. We did not detect a significant modification in *CO* transcript levels, which kept the same expression patterns throughout LD in WT, *fk12-1* and overexpressing plants (Figure 2d, above). However, *FKBP12* overexpression caused a high increase in *FT* mRNA levels, particularly during the morning (ZT4-ZT8) (Figure 2d, below, solid line), as

CO expression is not modified, this hinted to a posttranslational modification of CO protein activity. On the contrary, the mutant *fk12-1* showed a slight decrease in *FT* expression particularly during the evening, when CO activates *FT* expression (Figure 2d, below, black dotted line), again revealing a possible posttranslational modification of CO activity. Consistent with a role of FKBP12 over CO activity, flowering time of *FKBP12* mutants and overexpressor were not significantly altered in SD (Figure S6a), a photoperiod condition in which CO is not expressed during the day and the protein is not detectable (Suárez-López *et al.*, 2001, Valverde *et al.*, 2004). Similarly, the SD 24 h mRNA expression profiles of *CO* in WT, *fk12-1* mutant and 35S:*FK* plants (Figure S6b, left) did not show any significant change, and this was reflected also in a very small and low expression of *FT* in the same conditions (Figure S6b, right).

To further characterize the effect of FKBP12 in CO protein activity, we isolated nuclei from Col-0, *fk12-5* and 35S:*FK* plants and detected CO and FKBP12 protein levels (Figure 3a). While FKBP12 protein presence in the nucleus was low in WT and *fk12-5* mutant nuclei, the nuclear presence of the protein in 35S:*FK* was very high (Figure 3a). In the same blots, the amount of the upper band of CO, which represents the phosphorylated, active form (Sarid-Krebs *et al.*, 2015) was clearly visible in the 35S:*FK* plants compared to *fk12-5* mutant and Col-0 (Figure 3a, above). When these bands were quantified in three replicates and plotted (Figure 3a, below left) a significant amount of the phosphorylated band could be detected in the 35S:*FK* compared to Col-0 and *fk12-5* mutant. Furthermore, when we plotted the ratio of upper phosphorylated CO to the lower unphosphorylated form, that represents the active composition of native CO (Sarid-Krebs *et al.*, 2015), there was a significant reduction in the mutant and an increase in the 35S:*FK* plants (Figure 3a, below right). Indeed, these differences were reflected in the amount of FT protein present in total extracts of these plants in LD at ZT4 (Figure 3b), with *fk12-1* and *fk12-5* (Figure S7e) mutants showing a significant decrease in FT levels and different 35S:*FK* transformants showing a significant increase compared to Col-0 (Figure 3b, right and S4d). In these blots FKBP12 presence in Col-0 total extracts was always higher than in nuclei extracts indicating a preferred non-nuclear localization as shown in the confocal images of FK-CFP before (Figure S2a), while in 35S:*FK* plants FKBP12 was very abundant in both localizations.

At phenotypical level, we checked *FKBP12* mutants and overexpressor plants in LD, for a modification of flowering time in *Arabidopsis* (Figure 3c). Indeed, plants overexpressing *FKBP12* showed a significant small acceleration of flowering time, while *fk12*-1 and *fk12-5* mutants showed a small but significant late flowering phenotype in LD (Figure 3c, middle). WT plants flowered in LD at an average of 15.3 leaves, while *fk12-1* plants flowered with 17.1 leaves, *fk12-5* with 18.6 and 35S:*FK* with 13.0 leaves, both with a high degree of significance (Figure 3c, below). Therefore, while Col-0 plants were starting to bolt 21 days after germination (DAG), the immunophilin overexpressor was already fully bolting and the mutants had not yet flowered (Figure 2c, above).

To better characterize at genetic level *CO* and *FKBP12* interaction, we crossed plants overexpressing *CO* (35S:*CO:TAP, Ortiz et al., 2014),* and *fk12-1* plants. During the F1 segregation we scored the flowering time of the plants in LD and compared with the flowering time of the parental plants and Col-0 (Figure S7a). As expected for a regular Mendelian distribution, flowering time of the F1 population showed a three modal disposition showing a clear displacement of flowering time of the 35S:*CO*:*TAP* plants to the late flowering phenotype. Indeed, when we transformed 35S:*CO* constructs (Lucas-Reina *et al.*, 2015) into *fk12-1* mutant background, selected for *CO* overexpression vector resistance (BASTA) and sowed in soil a mixture of six T1 independent transformant seeds, a displacement of flowering time of the T2 population plants to a late flowering phenotype was also observed (Figure S7b). This was again consistent with a delay in the early flowering phenotype of *CO* overexpression caused by *FKBP12* absence, which could also be observed in the floral phenotype of the homozygous plants in LD (Figure S7c) 35S:*CO fk12-1* flowered with 14.7 leaves, *fk12-1* with 19.8 leaves and 35S:*CO* with 8.9 leaves. In fact, total protein extracts of 35S:*CO fk12-1* plants showed a significant increase in CO protein when compared to the single mutant, but the distribution of phosphorylated to unphosphorylated form was lower (Figure S7d) than in 35S:*CO* plants (compare with Figure 1e).

CO protein is stabilized by FKBP12

FKBP immunophilins can function as proline cis-trans isomerases and as molecular chaperones that help stabilize proteins and facilitate their intracellular movement

(Geisler & Bailly, 2007; Gollan *et al.*, 2012). CO is strongly influenced by several different posttranslational modifications, so that its final structure is likely to be important for its function and stability (Valverde *et al.*, 2004). To find out the effect of FKBP12 on CO stability we expressed again both proteins in *E. coli* using pETDuet-1 vector but this time as a His tagged CO (H·CO) and an S·tagged FKBP12 (S·FK). We observed that the lack of the immunophilin produced no effect on CO amount in total cell crude lysates (Figure 4a, left), but significantly reduced the amount of CO in soluble fractions when absent (Figure 4a, right), indicating that CO solubility was enhanced by FKBP12 presence.

In human cells, interaction of FKBP12 with TOR kinase depends on the macrolide drug rapamycin (Sirolimus) that forms a strong molecular bridge between the immunophilin and the kinase, inhibiting its phosphorylating activity (Shimobayashi & Hall, 2014). Other drugs, such as FK506 (Tacrolimus) can strongly bind human FKBP12 and influence the interaction with calcineurin phosphatase, inhibiting T-lymphocyte calcium-dependent signal transduction such as the transcription of *interleukin*-2 (Liu *et al.*, 1991). It has been shown that plant rapamycin does not form a molecular bridge between TOR and FKBP12 (Menand *et al.*, 2002) rendering plants immune to rapamycin, but no experiment with other drugs and targets has been performed. Both rapamycin (Rap) or FK506 seemed to have no effect on single H·CO retention in a cobalt column (Figure 4b, left). When we incubated protein extracts from H·CO/S·FK-producing bacteria with rapamycin, run the extract through the column, washed and eluted, again no difference in either FKBP12 retention or CO stability was detected in immunoblots (Figure 4b, middle, Rap). Nevertheless, when the same extracts were incubated with FK506, H·CO could not bind to the column with the same affinity (Figure 4b middle; right, FK506) and very little S·FK co-eluted with H·CO. In fact, S·FK was eluted in the washing steps (not shown). These results suggest that while rapamycin does not bind *Arabidopsis* FKBP12, and therefore, does not affect CO interaction, this is not the case with FK506 that seems to bind FKBP12 and interfere with CO interaction, although a deeper biochemical characterization would be needed to confirm this point.

CO protein has three distinct domains (Figure S8a), the two amino terminal b-boxes are involved in protein-protein interaction, the middle part in transcriptional activation and the C terminal domain (CCT) in nuclei import as well as DNA and protein

interactions (Wenkel *et al.*, 2006; Tiwari *et al.*, 2010). In order to identify CO domains involved in FKBP12 interaction, we performed Y2H assays. We cloned the three parts of CO in bait vector pJG4-5 and FKBP12 complete ORF in the prey vector pEG202. The resulting yeast growth and X-Gal assay (see experimental procedures) showed that FKBP12 strongly interacted with the CCT part of CO, while very weak interaction was observed with the amino and middle domains of the protein (Figure 4c). These results were repeated in transient BiFC assays in *Nicotiana* in which we co-transformed the amino terminal part of YFP fused to these same domains and the fusion of carboxy-terminal YFP with FKBP12 (Figure 4d and S9a, c-e). As expected, a strong YFP nuclear-cytosolic signal was observed under the confocal microscopy with the CCT part of CO (Figure 4d, rightmost panel) and only a weak one with the middle domain and the b-boxes (Figure 4d, left and middle panels). The finding suggested that FKBP12-CO interaction occurred mainly through the carboxyl terminal domain, which has been proposed to interact with E3 ligase COP1 and DNA (Jang et al, 2008; Tiwari *et al.*, 2010). As CO interaction with Pseudo Response Regulators (PRRs) has been also proposed to involve this domain (Hayama *et al.*, 2017), it suggests that CO could bind in a supramolecular complex to DNA and FKBP12, affecting this complex formation or stabilization.

Mapping CO-FKBP12 protein interaction

FKBP12 belongs to a family of prolyl-cis-trans isomerases involved in modifying proline topology within the polypeptide chain (Gollan *et al.*, 2012). CO amino acid sequence shows the conservation of three valine-proline pairs (Figure S8a, red VP, above), which are particularly well conserved into a subclade of the CO phylogenetic tree (Figure S8b, C). This clade contains CO orthologues from *Chlamydomonas* (CrCO), *Physcomitrella patens* (PpCOL1-3) and *Arabidopsis* (AtCOL1-5) (Serrano *et al.*, 2009; Valverde 2011) and constitute a set of CO-like proteins (COLs) whose function has been conserved throughout the green plants phylogenetic tree (Figure S8b, red clade). Due to their high conservation in the evolutionary history of COL proteins, prolines in these VP pairs were good candidates to be targeted by FKBP12 activity in order to modify CO structure. Therefore, we produced a modified CO* with prolines 215, 266 and 371 substituted by alanines (Figure S8a, below, VA).

First, when we co-expressed H·CO* with S·FK using pETDuet-1 vector in *E. coli*, the mutant protein showed a marked reduction in solubility compared to the native version (Figure 5a). The amount of CO protein in soluble extracts from bacteria producing the native H·CO protein and S·FK was significantly reduced (around 60%) in immunoblots when H·CO* was expressed together with S·FK compared to WT H·CO protein (Figure 5a, 2nd panel). This was not due either to a reduction of CO protein in cell crude lysates (Figure 5a, 1st panel), neither to a reduced FKBP12 presence, which was found to be equivalent in both extracts (Figure 5a, 3rd panel). Next, we performed transient BiFC assays in tobacco cells between CO* - FKBP12 and again the interaction differed to that of wild type (Figure 5b and S9a-b, g). While CO-FKBP12 interaction showed a specific nuclear localization (Figure 5b, above), the CO*-FKBP12 YFP signal was delocalized (Figure 5b, below). Nevertheless, when we tested in Y2H the interaction between FKBP12 and the VP-VA mutated form of the CCT domain at the three prolines (CTT*, Figure S10) there was no significant difference between the interaction with the wild type domain. This could indicate either that a plant specific posttranslational modification of the CCT domain is not present in yeast (for example a phosphorylation event) or that although the stability of the protein and its cellular localization are compromised in the triple VA mutant, this is not due to a direct lack of interaction between FKBP12 and the prolines of the VP pairs.

FKBP12-CO interaction is conserved in microalgae

C. reinhardtii is a chlorophyte microalgae used as a model photosynthetic protist whose genome is fully sequenced and annotated (Merchant *et al*., 2007). *Chlamydomonas* has a single CO orthologue identified as CrCO, which is involved in the photoperiodic control of starch accumulation and synchronic reproduction, showing a nuclear localization (Serrano *et al.*, 2009). *Chlamydomonas* is sensitive to rapamycin, which acts as a bridge to inhibit TOR kinase through the irreversible interaction with CrFKBP12, promoting growth arrest (Crespo *et al.*, 2005). To test if the interaction we had found in *Arabidopsis* was conserved in algae, we first cloned *CrFKBP12* fused to *YFP* behind a constitutive promoter (p*Rbcs*/*Hsp90*:*CrFKBP12*:*YFP)* and transformed *Chlamydomonas* cells. Next, we used the nucleic acid dye (SYTO Blue 45, ThermoFisher) to report *in vivo* the presence of the nucleus (Lucas-Reina *et al.*, 2015). Observation of untransformed

Chlamydomonas treated with SYTO blue 45 under the confocal microscope showed a distinct blue fluorescence signal in the nucleus (Figure 6a, above). When algae carrying the p*Rbcs*/*Hsp90*:*CrFKBP12*:*YFP* construct were incubated with SYTO Blue 45 and observed under the confocal microscope both yellow and blue signals coincided, reporting the nuclear presence of FKBP12 in the alga (Figure 6a, below).

Finally, to show CrCO-CrFKBP12 interaction we performed BiFC experiments in *Nicotiana* epidermal cells, and an intense fluorescence signal both at the cytosol and the nuclear compartments was observed (Figure 6b, left and S9a-b, h-i). Similarly, we also tested the fluorescence complementation between *Arabidopsis* CO and *Chlamydomonas* CrFKBP12 (Figure 6b, middle) and, reciprocally, between *Chlamydomonas* CrCO and *Arabidopsis* AtFKBP12 (Figure 6b, right). Both combinations reported a strong signal, hinting to a conserved interrelation between algae and plants homologues and showing the probable conservation and importance of this interaction among photosynthetic eukaryotes.

DISCUSSION

CONSTANS activity is crucial to promote photoperiod-dependent flowering in *Arabidopsis* and in a significant number of plants from different taxonomical families (Yano *et al.*, 2000; Yang *et al.*, 2014; Kurokura *et al.*, 2017). *CO* is controlled at the expression level by the circadian clock through a set of clock-controlled TFs such as CYCLING DOF FACTORS (CDFs) and FLOWERING BHLHs (FBHs) that are central to its transcriptional regulation (Imaizumi *et al.*, 2005; Ito *et al.*, 2012). Besides, it has also been shown that control of its activity takes place at the posttranslational level (Shim *et al.*, 2017). In this sense, the regulation through photoreceptor-dependent degradation (Valverde *et al.*, 2004), the COP1/HOS1 E3-ubiquitin ligases stablishing the night/day degradation by the proteasome (Jang *et al.*, 2008; Lazaro *et al.*, 2012), the building of supramolecular complexes to bind DNA (Wenkel *et al.*, 2006) and the phosphorylation of its active form (Sarid-Krebs *et al.*, 2015) seem to be essential for its mechanism of action. Here, we report a different component of posttranscriptional control of CO stability mediated by the interaction with the chaperone immunophilin FKBP12. In this model (Figure 7), FKBP12 (yellow squares) would interact with CO (blue circle) stabilizing

441 the phosphorylated form in the nucleus. FKBP12 binding to CO CCT domain could
442 prevent its degradation by COP1 and be directed to DNA to trigger the expression of *FT*
443 (An *et al.*, 2004) to promote flowering.

444 Although FKBP12 has been extensively studied in yeast and animals for its
445 capacity to interact with the key growth kinase TOR through rapamycin, this interaction
446 does not occur in plants (Gollan *et al.*, 2012). It has been proposed that the presence of
447 an internal disulphide bridge between two conserved Cys residues, could be responsible
448 for the lack of interaction with plant TOR (Menand *et al.*, 2002) and the induction of
449 complex formation with new partners (Xu *et al.*, 1998). FKBP12 is also the target of the
450 immunosuppressant drug FK506 that inhibits calcineurim and blocks T-lymphocyte
451 transduction pathway (Liu *et al.*, 1991). In a plant scenario, we describe here a different
452 role for FKBP12 in which its interaction with CO would have an effect on flowering time
453 and would be disrupted by FK506. Although it has been shown that *Vicia faba* FKBP12
454 cannot constitute a stable union with FK506 and calcineurim (Xu *et al.*, 1998), in our case
455 FK506 seemed to have an effect on CO-FK506-FKBP12 ternary complex formation
456 (Figure 4b). Although more rigorous tests will be needed to confirm this point, we could
457 predict a scenario in which the addition of FKBP12 inhibitors could have a use in agro
458 industry to alter flowering time by affecting CO-FKBP12 interaction.

459 Disrupting CO-FKBP12 interaction would have an effect on CO stability that can
460 be also seen when we mutate key VP residues in CO sequence (Figure 5a-b). Interaction
461 with the E3 ubiquitin ligases that promote CO degradation has been proposed to occur
462 at the CCT domain (Lazaro *et al.*, 2015), the same domain that binds FKBP12 (Figure 4c,
463 d). On the other hand, the positive effect of *FKBP12* overexpression on CO stability *in*
464 *vivo* (Figure 1e) and on its capacity to activate *FT* expression, particularly in the morning
465 (Figures 2d, S7e), the induction of the phosphorylated band in the 35SFK plants (Figures
466 1e, 3a) and the reduction of this band in the single (Figure 3a) and 35S:*CO fk12-1* double
467 mutant (Figure S7d) strongly support the idea that CO-FKBP12 interaction may be
468 affecting the E3 ubiquitin interactions and promoting CO stabilization. However, our
469 data cannot discard a possible effect due to its prolyl isomerase activity or to the effect
470 over other TFs affecting flowering.

In *Picea wilsoni*, PwFKBP12 interacts with PwHAP5 (Yu *et al.*, 2011), a homologue of CO binding partners in the HAP2/HAP3/HAP5 complex in *Arabidopsis* (Wenkel *et al.*, 2009). This interaction is crucial for the correct elongation of the pollen tube. Nevertheless, PwHAP5-PwFKBP12 interaction does not occur in the nucleus and must be affecting other intercellular processes. Therefore, the interaction with CO would follow a different cellular mechanism such as stability and cellular localization. In fact, the only well characterized FKBP12 interactor in *Arabidopsis* is AtFIP37 (FKBP12 interacting protein 37 kD) whose mutation causes a strong delay in endosperm development and embryo arrest (Vespa *et al.*, 2004). In the same work, Vespa and colleagues mention that *fkbp12* mutant does not show any early developmental phenotype, but no deep description of the mutant, particularly at later stages, was shown. Therefore, we provide here a more complete developmental analysis in plant of a *fkbp12* mutant, and although indeed no embryo arrest or major growth failure has been detected, a closer inspection of its life cycle shows that *fk12* mutants are late flowering (Figure 3c). On the other hand, overexpression of *FKBP12* under a constitutive promoter triggered early flowering. Both mutant and overexpression lines had no effect on *CO* mRNA accumulation (Figure 2d), but did show an effect on CO protein presence in the nucleus (Figures 1e), particularly of the phosphorylated form (Figure 3a) hinting to a possible role on the posttranslational modification of CO activity. Correspondingly, the major target of CO, FT (Samach *et al.*, 2000), showed a clear reduced expression and abundance in *fk12* mutants, while FT presence was particularly high in 35S:*FK* plants (Figure 2b, 3b, S4d, S7e). In fact, in all *FKBP12ox* transformants, which are early-flowering plants, *FT* expression in the morning is very high, and indeed *FT* expression in 35S:*FK* shows a bimodal expression pattern, with a peak in the morning and a second in the evening (Figure 3d). Higher expression of *FT* in the morning has recently been reported in *Arabidopsis* plants grown in the wild and has been explained due to a higher increase in CO activity in the morning than that observed in laboratory conditions (Song *et al.*, 2018). Our results suggest likewise that *FKBP12* overexpression helps stabilize the upper, phosphorylated and activate form of CO protein in the morning, and this is reflected in a higher production of FT and subsequent early flowering phenotype. On the contrary, lack of FKBP12 protein will produce lower abundance of nuclear active CO

protein that would promote a reduction in *FT* expression in the evening and eventually a late-flowering phenotype.

It is also remarkable that CO-FKBP12 interaction is conserved in *Chlamydomonas*, as shown by BiFC experiments with CrCO and CrFKBP12 orthologues, (Figure 6b). Nevertheless, the interaction between both proteins showed a widespread nuclear-cytosolic distribution in *Nicotiana* cells, probably reflecting differences in cellular localization between algae and plants, although new nuclear import experiments would be needed to confirm this point. The confirmation of the CrCO-CrFKBP12 interaction in *Chlamydomonas* is in line with previous observations in which a conserved photoperiod response from algae to plants, sharing many common proteins, had been described (Serrano et al, 2009; Lucas-Reina *et al.*, 2015). These results confirm the importance of some conserved photoperiodic regulatory tools in the evolution of photosynthetic eukaryotes (Romero & Valverde, 2009; Serrano-Bueno *et al.*, 2017).

In conclusion, as depicted in the model of Figure 7, photoperiodic flowering control mediated by CO is modulated at posttranscriptional level by the interaction with the immunophilin FKBP12, facilitating the nuclear stability of the active form and *FT* transcription. Although we cannot discard other effects associated with FKBP12 derived from its prolyl isomerase activity or to the effect over other TFs involved in flowering time, CO-FKBP12 interaction seems highly conserved in the green lineage, and has a measurable effect on flowering time in plants, altogether unveiling a strong evolutionary importance.

EXPERIMENTAL PROCEDURES

Plant material and growth conditions

Arabidopsis thaliana L. Heynh. (thale cress) wild type were from Columbia (Col-0) ecotype. The T-DNA insertion mutant *fk12-1* (SALK_064494.47.85.x) was obtained from the SALK collection while the *fk12-5* mutant (WiscDsLox1E10) was obtained from the Wisconsin Collection. For 35S:*FK* lines, full-length cDNA (RIKEN) was cloned into a pEarlyGate 100 vector (Early *et al.*, 2006) behind the CaMV 35S promoter or in the cTapi.289.gw (Rohila *et al.*, 2004) to obtain the FK-TAP version. For each recombinant

plant at least ten individuals were initially isolated and finally three plants, showing a homogeneous phenotype, selected for the analysis. Plants were grown in controlled cabinets on peat-based compost (for flowering time determination, FRET and BiFC Assays) or in MS plates (for qRT-PCR assays and protein determinations). Seeds were previously incubated for 4 days at 4°C in the dark before sowing under LD cycles with temperatures ranging from 22°C (day) to 18°C (night).

Pull-down assays in bacteria

Full-length *CO* and *FKBP12* CDSs were cloned into pETDuet-1 vector (Novagen) and introduced into *E. coli* BL21 cells. S·tagged CO (S·CO)/His·tagged CO (H·CO) and His·tagged FKBP12 (H·FK)/S·tagged FKBP12 (S·FK) versions were induced 4 h with 1 mM isopropyl-β-thiogalactopyranoside (IPTG, Applichem) at 30˚C. S·CO was immobilized on protein A magnetic beads previously charged with S·tag antibody. For pull-down assays, H·FK was incubated with the immobilized S·CO for 2 h at 4˚C. Proteins were detected by immunoblot using αCO (raised in rabbit against CO middle domain as described in Valverde *et al.*, 2004), αFKBP12 (this work, see below), αFT (Agrisera) and αHis antibodies (Qiagen). Loading controls for nuclei extracts were histone 3 antibody (Abcam) and for cytosol extracts an antibody against recombinant non-phosphorylating GAPDH (GAPN) as described in Valverde *et al.*, 1999.

Yeast-based protein interaction analysis

Split-Ubiquitin System (SUS) was as in Pusch *et al.* 2012, using a cDNA library from Filipa Santos, Iris Ottenschläger and Klaus Palme (MPIZ, Cologne, Germany). CO was cloned in bait vector pMET-Cub-R-URA and cDNA in prey vector pCU-Nub and transformed into JD53 yeast strain. Cells were plated onto minimal SD medium plates +/- URA supplemented with 25 μM Met and 100 μM copper sulphate for growth control, or on SD plus 1 mg/ml FOA, 25 μM Met and 100 μM copper sulphate for clone rescue. Cells were grown at 30°C for 3 days, surviving clones identified, DNA rescued by plasmid extraction and tested by PCR. For Yeast-Two-Hybrid (Y2H) assays, CO domains CCT, CCT*, middle and Bbox domains were cloned into bait vector pJG4-5, while full-length *FKBP12* CDS was cloned into prey vector pEG202. Primers used to generate Y2H clones are listed in Table S1. EGY48 (MATα *trp1 ura3 his3 LEU2::pLex Aop6-LEU2*) was used as

the host strain for Y2H experiments (Gyuris *et al.*, 1993). Positive interactions were detected by blue color on Ura-His-Trp-X-gal plates and survival on GAL-Ura-Trp-His-Leu-selective plates. For quantitative assays, the transformants were grown at 30°C to 0.5–0.8 OD 600 nm. The β-gal activity (U/ml) in Figure 4c was measured by OD 420 nm using o-nitrophenyl β-d-galactopyranoside (Sigma).

Protein Analysis

Arabidopsis proteins were isolated from two-week DAG seedlings grown in MS plates employing the Trizol (Invitrogen) protocol as described by the manufacturer. Nuclear-enriched fractions were obtained from Col-0, 35S:*CO*, 35S:*FK*, *fk12-1*, *fk12-5,* 35S:*CO fk12-1* and 35S:*CO*:*TAP* tag (Ortiz *et al.*, 2014) seedlings grown in MS plates for two weeks as described (Lazaro *et al.*, 2012). *FKBP12*, *CO* and *CO** expressed in *E. coli* BL21 cells were induced as above. Cells were disrupted using glass beads (0.5 mm) in an extraction buffer containing 0.33 mM sorbitol, 25 mM Tris-HCl (pH 7.5), 2 mM EDTA, 2 mM DTT, 1 mM PMSF, 1 mM benzamidine, and 1 mM ϵ-aminocaproic acid and soluble fractions isolated by low speed (5 min, 500 *g*) followed by high speed (15 min, 20,000 *g*) centrifugations. Protein amount was determined by Bradford Bio-Rad assay according to the manufacturer's instructions with ovalbumin as a standard. Proteins were separated by SDS-PAGE using standard procedures, transferred to nitrocellulose or PVDF filters and probed with αCO, αFT or αFK. FKBP12 antibodies were raised in rabbit against the synthesized (Sigma) specific Arabidopsis FKBP12 peptide (NH3-MGEVIKGWDEGVAQMC-COOH) and further purified through column-bound FKBP12-Histag. αH3 (Abcam) was used as nuclear protein marker. Blots were developed with a chemiluminescent substrate according to the manufacturer's instructions (Immobilon Western Chemiluminescent HRP Substrate; Millipore).

Co-immunoprecipitation experiments were performed by transient assays in *Nicotiana* cells as described in Lazaro *et al.* 2015. In brief, *Agrobacterium* transformed with 35S:*FKBP12*:*TAP* (FK-TAP), 35S:*CO*:*YFP* (CO-YFP) or combination of both, were infiltrated in young leaves of *Nicotiana* as described below. After three days, 1 g of infected tissue or negative control (only p19) was grinded with mortar and pestle in the presence of liquid nitrogen and resuspended in 2 ml co-IP buffer (Lazaro *et al.*, 2015).

After centrifugation for 10 min at 5,000 rpm in a microfuge at 4°C, 0.5 ml of supernatants were incubated with 25 µl washed GFP-Trap®_MA nanobody beads (Chromotek) and stirred for 2 h at 4°C in a rotor incubator. After three washes in co-IP buffer, samples were eluted by adding 5X SDS-PAGE loading buffer and incubating at 95°C for 5 min.

Microscopy

For Bi-molecular Fluorescence Complementation (BiFC) experiments, *FKBP12*, different domains of *CO* and their *Chlamydomonas* orthologues were cloned in pYFN43 and pYFC43 vectors (Ferrando *et al.*, 2001) to produce N-terminal fusions of the carboxyl (pYFC43) and amino (pYFN43) parts of YFP. These constructs were introduced into *A. tumefaciens* strain C58 and infiltrated in *Nicotiana* leaves together with p19 protein (Voinnet *et al.*, 2003). BiFC protocol was followed as previously described (Lucas-Reina *et al.*, 2015). Amino and carboxyl domains of AKINβ and AKIN10 Sucrose-non-fermenting (Snf1)-related kinases (SnRK) were used as positive control (Ferrando *et al.*, 2001). Co-agroinfiltrations with empty vectors were used as negative controls. BiFC was visualized under a Leica TCS SP2 confocal microscopy set at 550 nm and analyzed with Leica LCSLite software. For FRET experiments, CO-YFP and FK-CFP constructs were introduced in *Nicotiana* leaves by agroinfiltration. 2-3 days after transfection, epidermal cells were visualized using a Leica TCS SP2/DMRE microscope equipped with a 63x objective lens. CFP was excited with a 458 nm laser and YFP with a 514 nm laser. Band-pass filters were adjusted to 465-479 nm and 520-545 nm in the CFP and YFP detection channels, respectively. FRET was measured by the acceptor photobleaching technique, thus, regions of interest (ROIs) were bleached using the argon-ion laser at high intensity to remove fluorescence of acceptor. 10 cell nuclei were imaged to quantify the change in donor fluorescence and FRET efficiency was measured according to the formula: (pre-bleaching - post-bleaching) / (pre-bleaching). For *C. reinhardtii* nuclear transformation, an electroporation protocol was used (Lucas-Reina *et al.,* 2015). CW15 and several *CrFKBP12*:*YFP* transgenic lines were observed under the confocal microscope together with SYTOBlue45 Fluorescent Nucleic Acid Stain (Molecular Probes). Algae were grown in SD conditions in Sueoka medium supplemented with 10 mM NO_3– until lag phase (3–4 µg ml^{-1} Chlorophyll). 1 ml was collected by centrifugation (4 min, 5,500g) and suspended in 1 ml Tris-buffered saline (TBS) buffer. 1 µl SYTOBlue45

and 1 and 5 µl of 10% (v/v) Triton X-100 for CW15 cells and transgenic lines, respectively, were added. After incubation for 10 min, cells were centrifuged and suspended in 100 µl of the same buffer. Finally, 3 µl of cells were mixed with 10 µl of 1.2% (w/v) low point fusion agarose at 30°C. Wavelengths used were 514 nm for YFP and 458 nm for SYTOBlue45.

RNA Extraction and qRT-PCR

1 µg of Trizol-isolated RNA was used to synthesize cDNA with the Quantitec Reverse Kit (Qiagen) following manufacturer instructions and diluted to a final concentration of 10 ng/µl. Primers for *CO*, *FT* and *UBQ10* amplification (Ortiz-Marchena *et al.,* 2014) were used in an iQTM5 multicolor real-time PCR detection system (Bio-Rad) in a 10-µl reaction: primers 0.2 µM, 10 ng cDNA, 5 µl SensiFAST TM from SYBR Fluorescein kit (Bioline). Initial concentration of candidate and reference genes was calculated by means of LingRegPCR software version 11.0 (Ruijter *et al.*, 2009). Normalized data were calculated by dividing the average of at least three replicates of each sample from the candidate and reference genes.

Analysis of Flowering Time

Flowering time was analyzed in controlled-environment cabinets by scoring the number of rosette (excluding cotyledons) and cauline leaves. Data are from media of at least 20 individuals ± s.e.

Site-directed mutagenesis

Site-directed mutagenesis was performed to replace the conserved VP pairs of CO to VA pairs according to the manufacturer's instructions (Muta-direct™ Site-Directed Mutagenesis, iNtRON Biotechnology). All constructs were verified by DNA sequencing. Primers used are listed in table S1.

Statistical Analysis

The statistical data are marked with asterisks and are means ± s.e. of at least three biological experiments. The statistical significance between means of the different

samples was calculated using a two-tailed Student's t test. Differences observed were considered statistically significant at $P < 0.05$ (*), $P < 0.01$ (**), and $P < 0.001$ (***).

ACKNOWLEDGEMENTS

Funding from projects BIO2014-52425-P, BIO2017-83629-R (Spanish Ministry of Science) and P08-AGR-03582, BIO-281 (Junta de Andalucia) supported by FEDER funding, is acknowledged. GS-B received financial support from the European Union project H2020-MSCA-IF-2018, GA838317. FES received a Spanish Ministry of External Affairs (AECID) fellowship and EIL-R a CSIC-JAE fellowship, partly supported by structural funding from the EU (SEF). The IBVF microscopy services (Alicia Orea) and University of Seville microscopy and glasshouse services (General Research Services, CITIUS) are also acknowledged. All authors declare that there is no conflict of interest in the publication of this article.

AUTHOR CONTRIBUTION

GS-B and FES produced most of the results data, wrote text and made figures; PdlR did most of the QPCR, FRET, statistics and bioinformatics data; EIL-R produced the mutagenesis and bacterial biochemistry experiments; MIO-M produced the flowering time data and mutant analysis; JMR and FV procured funding, designed and reviewed experimental procedures, wrote the text and corrected the different versions of the manuscript.

DATA STATEMENT

All materials, figures and supporting data are available upon request from the corresponding author at federico.valverde@ibvf.cscic.es

SUPPORTING INFORMATION

Additional Supporting Information is available in the online version of this article:

Figure S1. Classification of CO interactors.
Figure S2. Subcellular localization of CO and FKBP12.
Figure S3. CONSTANS-FKBP12 interaction *in vivo*.
Figure S4. Characterization of *fkbp12* mutants.
Figure S5. Analysis of *FKBP12* circadian expression.
Figure S6. Flowering time, *CO* and *FT* expression in SD.

679 **Figure S7.** Characterization of the genetic interaction between *CO* and *FKBP12*.
680 **Figure S8.** Conserved Valine-Proline (VP) residues and phylogenetic tree of COL proteins.
681 **Figure S9.** BiFC controls.
682 **Figure S10.** Interaction between CO* and FKBP12.
683 **Table S1.** List of primers used in this work.
684 **REFERENCES**

685 - **An, H., Roussot, C., Suárez-López, P., Corbesier, L., Vincent, C., Pineiro, M., Hepworth,**
686 **S., Mouradov, A., Justin, S., Turnbull, C., *et al.*** (2004) CONSTANS acts in the phloem to
687 regulate a systemic signal that induces photoperiodic flowering of Arabidopsis.
688 *Development* **131**, 3615-3626.

689 - **Andrés, F. and Coupland, G.** (2012) The genetic basis of flowering responses to
690 seasonal cues. *Nat. Rev. Genet.* **13**, 627-639.

691 - **Austen, E.J., Rowe, L., Stinchcombe. J.R. and Forrest, J.R.K.** (2017) Explaining the
692 apparent paradox of persistent selection for early flowering. *New Phyt.* **215**, 929-934.

693 - **Ben-Naim, O., Eshed, R., Parnis, A., Teper-Bamnolker, P., Shalit, A., Coupland, G.,**
694 **Samach, A. and Lifschitz, E.** (2006) The CCAAT binding factor can mediate interactions
695 between CONSTANS-like proteins and DNA. *Plant J.* **46**, 462-76.

696 - **Blümel, M., Dally, N. and Jung, C.** (2015) Flowering time regulation in crops – what did
697 we learn from Arabidopsis? *Cur. Opin. Biotech.* **32**, 121-129.

698 - **Cyert, M.S.** (2001) Regulation of Nuclear Localization during Signaling. *J. Biol. Chem.*
699 **276**, 20805-20808.

700 - **Crespo, J.L., Díaz-Troya, S. and Florencio, F.J.** (2005) Inhibition of target of rapamycin
701 signalling by rapamicin ib the unicellular green alga *Chlamydomonas reinhardtii*. *Plant*
702 *Phys.* **139**, 1736-1749.

703 - **Dünnwald, M., Varshavsky, A. and Johnsson, N.** (1999) Detection of transient in vivo
704 interactions between substrate and transporter during protein translocation into the
705 endoplasmic reticulum. *Mol. Biol. Cell* **10**, 329-344.

- **Earley, K.W., Haag, J.R., Pontes, O., Opper, K., Juehne, T., Song, K. and Pikaard, C.S.** (2006) Gateway-compatible vectors for plant functional genomics and proteomics. *Plant J.* **45**, 616-629.

- **Edgar, R.C.** (2004) MUSCLE: multiple sequence alignment with high accuracy and high throughput. *Nucleic Acids Res.* **32**, 1792-1797.

- **Faure, J.D., Gingerich, D. and Howell, S.H.** (1998). An Arabidopsis immunophilin, AtFKBP12, binds to AtFIP37 (FKBP interacting protein) in an interaction that is disrupted by FK506. *Plant J.* **15**, 783-789.

- **Ferrando, A., Koncz-Kalman, Z., Farras, R., Tiburcio, A., Schell, J. and Koncz, C.** (2001) Detection of in vivo protein interactions between Snf1-related kinase subunits with intron-tagged epitope-labelling in plants cells. *Nucleic Acids Res.* **29**, 3685-3693.

- **Geisler, M. and Bailly, A.** (2007) Tête-à-tête: the function of FKBPs in plant development. *Trends Plant Sci.* **12**, 465-473.

- **Gnesutta, N., Kumimoto, R.W., Swain, S., Chiara, M., Siriwardana, C., Horner, D.S., Holt III, B.F., and Mantovani, R.** (2017) CONSTANS Imparts DNA Sequence Specificity to the Histone Fold NF-YB/NF-YC Dimer. *Plant Cell* **29**, 1516-1532.

- **Gollan, P.J., Bhave, M. and Aro, E.-M.** (2012) The FKBP families of higher plants: Exploring the structures and functions of protein interaction specialists. *FEBS Let.* **586**, 3539-3547.

- **Guo, X., Yu, C., Luo, L., Wan, H., Zhen, N., Xu, T., Tan, J., Pan, H. and Zhang, Q.** (2017) Transcriptome of the floral transition in *Rosa chinensis* 'Old Blush'. *BMC Genomics* **18**, 199.

- **Gyuris, J., Golemis, E., Chertkov, H. and Brent, R.** (1993) Cdi1, a human G1 and S phase protein phosphatase that associates with Cdk2. *Cell* **75**, 791-803.

- **Hayama, R., Sarid-Krebs, L., Richter, R., Fernández, V., Jang, S. and Coupland, G.** (2017) PSEUDO RESPONSE REGULATORs stabilize CONSTANS protein to promote flowering in response to day length. *EMBO J.* **36**, 904-918.

- **Hu, Y., Chen, L., Wang, H., Zhang, L., Wang, F and Yu, D.** (2013) *Arabidopsis* transcription factor WRKY8 functions antagonistically with its interacting partner VQ9 to modulate salinity stress tolerance. *Plant J.* **74**, 730–745.

- **Igarashi, D., Ishida, S., Fukazawa, J. and Takahashi, Y.** (2001) 14-3-3 Proteins Regulate Intracellular Localization of the bZIP Transcriptional Activator RSG. *Plant Cell* **13**, 2483-2498.

- **Imaizumi, T., Schultz, T.F., Harmon, F.G., Ho, L.A. and Kay, S.A.** (2005) FKF1 F-box protein mediates cyclic degradation of a repressor of CONSTANS in Arabidopsis. *Science* **309**, 293-297.

- **Ito, S., Song, Y.H., Josephson-Day, A.R., Miller, R.J., Breton, G., Olmstead, R.G. and Imaizumi, T.** (2012) FLOWERING BHLH transcriptional activators control expression of the photoperiodic flowering regulator CONSTANS in Arabidopsis. *Proc. Natl. Acad. Sci. USA* **109**, 3582-3587.

- **Jackson, S.D.** (2009) Plant responses to photoperiod. *New Phytol.* **181**, 517-531.

- **Jang, S., Marchal, V., Panigrahi, K.C.S., Wenkel, S., Soppe, W., Deng, X.W., Valverde, F. and Coupland, G.** (2008) Arabidopsis COP1 shapes the temporal pattern of CO accumulation conferring a photoperiodic flowering response. *EMBO J.* **27**, 1277-1288.

- **Johnsson, N. and Varshavsky, A.** (1994) Split ubiquitin as a sensor of protein interactions in vivo. *Proc. Natl. Acad. Sci. USA* **91**, 10340-10344.

- **Jakoby, M.J., Weinl, C., Pusch, S., Kuijt, S.J., Merkle, T., Dissmeyer, N. and Schnittger, A.** (2006) Analysis of the subcellular localization, function, and proteolytic control of the Arabidopsis cyclin-dependent kinase inhibitor ICK1/KRP1. *Plant Physiol.* **141**, 1293-1305.

- **Kang, C.B., Hong, Y., Dhe-Paganon, S. and Yoon, H.-S.** (2008) FKBP family proteins: immunophilins with versatile biological functions. *Neurosignals* **16**, 318-325.

- **Karpova, T.S., Baumann, C.T., He, L., Wu, X., Grammer, A., Lipsky, P., Hager, G.L. and McNally, J.G.** (2003) Fluorescence resonance energy transfer from cyan to yellow

759 fluorescent protein detected by acceptor photobleaching using confocal microscopy and
760 a single laser. *J. Microsc.* **209**, 56-70.

761 - **Kim J.E. and Chen, J.** (2002) Cytoplasmic–nuclear shuttling of FKBP12-rapamycin-
762 associated protein is involved in rapamycin-sensitive signaling and translation initiation.
763 *Proc. Natl. Acad. Sci. USA* **97**, 14340-14345.

764 - **Kodama, Y.** (2011) A bright green-colored bimolecular fluorescence complementation
765 assay in living plant cells. *Plant Biotech.* **28**, 95-98.

766 - **Kurokura, T., Samad, S., Koskela, E., Mouhu, K. and Hytönen, T.** (2017) *Fragaria vesca*
767 CONSTANS controls photoperiodic flowering and vegetative development. *J. Exp. Bot.*
768 **68**, 4839-4850.

769 - **Laubinger, S., Marchal, V., Gentilhomme, J., Wenkel, S., Adrian, J., Jang, S., Kulajta,**
770 **C., Braun, H., Coupland, G. and Hoecker, U.** (2006) Arabidopsis SPA proteins regulate
771 photoperiodic flowering and interact with the floral inducer CONSTANS to regulate its
772 stability. *Development* **133**, 4608-4608.

773 - **Lazaro, A., Valverde, F., Piñeiro, M. and Jarillo, J.A.** (2012) The E3 ubiquitin ligase
774 HOS1 participates in the control of photoperiodic flowering in Arabidopsis negatively
775 regulating CONSTANS abundance. *Plant Cell* **24**, 982-999.

776 - **Lazaro, A., Mouriz, A., Piñeiro, M. and Jarillo, J.A.** (2015) Red light-mediated
777 degradation of CONSTANS by the E3 ubiquitin ligase HOS1 regulates photoperiodic
778 flowering in Arabidopsis. *Plant Cell* **27**, 2437-2454.

779 - **Levin, D.** (2009) Flowering-time plasticity facilitates niche shifts in adjacent
780 populations. *New Phytol.* **183**, 661-666.

781 - **Liu, J., Farmer, J., Lane, W., Friedman, J., Weissman, I. and Schreiber, S.** (1991)
782 Calcineurin is a common target of cyclophilin-cyclosporin A and FKBP-FK506 complexes.
783 *Cell* **66**, 807-815.

- **Loewith, R., Jacinto, E., Wullschleger, S., Lorberg, A., Crespo, J.L., Bonenfant, D., Oppliger, W., Jenoe, P. and Hall, M.N.** (2002) Two TOR complexes, only one of which is rapamycin sensitive, have distinct roles in cell growth control. *Mol. Cell* **10**, 457-468.

- **Lucas-Reina, E., Romero-Campero, F.J., Romero, J.M. and Valverde, F.** (2015) An Evolutionarily Conserved DOF-CONSTANS Module Controls Plant Photoperiodic Signalling. *Plant Physiol.* **168**, 561-574.

- **Mathieu, J., Warthmann, N., Küttner, F. and Schmid, M.** (2007) Export of FT Protein from Phloem Companion Cells Is Sufficient for Floral Induction in *Arabidopsis*. *Cur. Biol.* **17**, 1055-1060.

- **Mattioli, R., Falascb, G., Sabatini, S., Altamura, M.M., Costantino, P. and Trovato, M.** (2009) The proline biosynthetic genes *P5CS1* and *P5CS2* play overlapping roles in *Arabidopsis* flower transition but not in embryo development. *Physiol. Plant.* **137**, 72-85.

- **Meiri, D., Tazat, K., Cohen-Peer, R., Farchi-Pisanty, O., Aviezer- Hagai, K., Avni and A., Breiman, A.** (2010) Involvement of Arabidopsis ROF2 (FKBP65) in thermotolerance. *Plant Mol. Biol.* **72**, 191-203.

- **Menand, B., Desnos, T., Nussaume, L., Berger, F., Bouchez, D., Meyer, C. and Robaglia, C.** (2002) Expression and disruption of the Arabidopsis TOR (target of rapamycin) gene. *Proc. Natl. Acad. Sci. USA* **99**, 6422-6427.

- **Merchant, S.S., Prochnik, S.E., Vallon, O., Harris, E.H., Karpowicz, S.J., Witman, G.B., Terry, A., Salamov, A., Fritz-Laylin, L.K., Maréchal-Drouard, L., *et al.*** (2007) The Chlamydomonas genome reveals the evolution of key animal and plant functions. *Science* **318**, 245-250.

- **Onouchi, H., Igeño, M.I., Perilleux, C., Graves, K. and Coupland, G.** (2000) Mutagenesis of plants overexpressing CONSTANS demonstrates novel interactions among *Arabidopsis* flowering-time genes. *Plant Cell* **12**, 885-900.

- **Ortiz-Marchena, M.I., Albi, T., Lucas-Reina, E., Said, F.E., Romero-Campero, F.J., Cano, B., Ruiz, M.T., Romero, J.M. and Valverde, F.** (2014) Photoperiodic control of carbon distribution during the floral transition in Arabidopsis. *Plant Cell* **26**, 565-584.

- **Ortiz-Marchena, M.I., Romero, J.M. and Valverde, F.** (2015) Photoperiodic control of sugar release during the floral transition: What is the role of sugars in the florigenic signal? *Plant Signal. Behav.* **5**, e1017168.

- **Pajoro, A., Biewers, S., Dougali, E., Leal Valentim, F., Mendes, M.A., Porri, A., Coupland, G., Van de Peer, Y., van Dijk, A.D., Colombo, L. *et al.*** (2014) The (r)evolution of gene regulatory networks controlling Arabidopsis plant reproduction: a two-decade history. *J. Exp. Bot.* **65**, 4731-4745.

- **Posé, D., Verhage, L., Ott, F., Yant, L., Mathieu, J., Angenent, G.C., Immink, R.G. and Schmid, M.** (2013) Temperature-dependent regulation of flowering by antagonistic FLM variants. *Nature* **503**, 414-417.

- **Pusch, S., Harashima, H. and Schnittger, A.** (2012) Identification of kinase substrates by bimolecular complementation assays. *Plant J.* **70**, 348-356.

- **Rohila, J.S., Chen, M., Cerny, R. and Fromm, M.E.** (2004) Improved tandem affinity purification tag and methods for isolation of protein heterocomplexes from plants. *Plant J*. **38**, 172–181

- **Romero, J.M. and Valverde, F.** (2009) Evolutionarily conserved photoperiod mechanisms in plants. When did plant photoperiodic signalling appear? *Plant Sig. Behav.* **4**, 642-644.

- **Ruijter, J.M., Ramakers, C., Hoogaars, W.M., Karlen, Y., Bakker, O., van den Hoff, M.J. and Moorman, A.F.M.** (2009) Amplification efficiency: Linking baseline and bias in the analysis of quantitative PCR data. *Nucleic Acids Res.* **37**, e45.

- **Samach, A., Onouchi, H., Gold, S.E., Ditta, G.S., Schwarz-Sommer, Z., Yanofsky, M.F. and Coupland, G.** (2000) Distinct roles of CONSTANS target genes in reproductive development of Arabidopsis. *Science* **288**, 1613-1616.

- **Sarid-Krebs, L., Panigrahi, K.C.S., Fornara, F., Takahashi, Y., Hayama, R., Jang, S., Tilmes, V., Valverde, F. and Coupland, G.** (2015) Phosphorylation of CONSTANS and its COP1-dependent degradation during photoperiodic flowering of Arabidopsis. *Plant J.* **84**, 451-463.

- **Serrano, G., Herrera-Palau, R., Romero, J.M., Serrano, A., Coupland, G. and Valverde, F.** (2009) Chlamydomonas CONSTANS and the evolution of plant photoperiodic signaling. *Curr. Biol.* **19**, 359-368.

- **Serrano-Bueno, G., Romero-Campero, F.J., Lucas-Reina, E. Romero, J.M. and Valverde, F.** (2017) Evolution of photoperiod sensing in plants and algae. *Curr. Opin. Plant Biol.* **37**, 10-17.

- **Shim, J.S., Kubota, A. and Imaizumi, T.** (2017) Circadian Clock and Photoperiodic Flowering in Arabidopsis: CONSTANS Is a Hub for Signal Integration. *Plant Phys.* **173**, 5-15.

- **Shimobayashi, M. and Hall, M.N.** (2014) Making new contacts: the mTOR network in metabolism and signalling crosstalk. *Nat. Rev. Mol. Cell Biol.* **15**, 155-162.

- **Song, J., Angel, A., Howard, M. and Dean, C.** (2012) Vernalization - a cold-induced epigenetic switch. *J. Cell Sci.* **125**, 3723-3731.

- **Song, Y.H., Kubota, A., Covington, M.F., Lee, N. *et al.*** (2018) Molecular basis of flowering under natural long-day conditions in *Arabidopsis*. *Nat. plants* **4**, 824-835.

- **Suárez-López, P., Wheatly, K., Robson, F., Onouchi, H., Valverde, F. and Coupland, G.** (2001) CONSTANS mediates between the circadian clock and the control of flowering in Arabidopsis. *Nature* **410**, 4116-4120.

- **Swiezewski, S., Liu, F., Magusin, A. and Dean, C.** (2009) Cold-induced silencing by long antisense transcripts of an Arabidopsis Polycomb target. *Nature* **462**, 799-802.

- **Tamura, K., Stecher, G., Peterson, D., Filioski, A. and Kumar, S.** (2013) MEGA6: Molecular Evolutionary Genetics Analysis Version 6.0. *Mol. Biol. Evol.* **30**, 2725-2729.

- **Tiwari, S.B., Shen, Y., Chang, H.C., Hou, Y., Harris, A., Ma, S.F., McPartland, M., Hymus, G.J., Adam, L., Marion, C., *et al.*** (2010) The flowering time regulator CONSTANS is recruited to the FLOWERING LOCUS T promoter via a unique cis-element. *New Phytol.* **187**, 57-66.

- **Valverde, F., Losada, M. and Serrano, A.** (1999) Engineering a central metabolic pathway: glycolysis with no net phosphorylation in an *Escherichia coli gap* mutant complemented with a plant *GapN* gene. *FEBS Lett* **449**, 153-158.

- **Valverde, F., Mouradov, A., Soppe, W., Ravenscroft, D., Samach, A. and Coupland, G.** (2004) Photoreceptor regulation of CONSTANS protein in photoperiodic flowering. *Science* **303**, 1003-1006.

- **Valverde, F.** (2011) CONSTANS and the evolutionary origin of photoperiodic timing of flowering. *J. Exp. Bot.* **62**, 2453-2463.

- **Vespa, L., Vachon, G., Berger, F., Perazza, D., Faure, J.-D. and Herzog, M.** (2004) The Immunophilin-Interacting Protein AtFIP37 from Arabidopsis Is Essential for Plant Development and Is Involved in Trichome Endoreduplication. *Plant Phys.* **134**, 1283-1292.

- **Voinnet, O., Rivas, S., Mestre, P. and Baulcombe, D.** (2003) An enhanced transient expression system in plants based on suppression of gene silencing by the p19 protein of tomato bushy stunt virus. *Plant J.* **33**, 949-956.

- **Wenkel, S., Turck, F., Singer, K., Gissot, L., Le Gourrierec, J., Samach, A. and Coupland, G.** (2006) CONSTANS and the CCAAT box binding complex share a functionally important domain and interact to regulate flowering of Arabidopsis. *Plant Cell* **18**, 2971-2984.

- **Wilson, R.S., Swatek, K.N. and Thelen, J.J.** (2016) Regulation of the Regulators: Post-Translational Modifications, Subcellular, and Spatiotemporal Distribution of Plant 14-3-3 Proteins. *Front. Plant Sci.* **7**, 611.

- **Xiong, Y. and Sheen, J.** (2012) Rapamycin and Glucose-Target of Rapamycin (TOR) Protein Signaling in Plants. *J. Biol. Chem.* **287**, 2836-2842.

- **Xu, Q., Liang, S., Kudla, J. and Luan, S.W.** (1998) Molecular characterization of a plant FKBP12 that does not mediate action of FK506 and rapamycin. *Plant J.* **15**, 511-519.

- **Yang, S., Weers, B.D., Morishige, D.T. and Mullet, J.E.** (2014) CONSTANS is a photoperiod regulated activator of flowering in sorghum. *BMC Plant Biol.* **14**, 148.

- **Yano, M., Katayose, Y., Ashikari, M., Yamanouchi, U., Monna, L., Fuse, T., Baba, T., Yamamoto, K., Umehara, Y., Nagamura, Y. and Sasaki, T.** (2000) Hd1, a major photoperiod sensitivity quantitative trait locus in rice, is closely related to the Arabidopsis flowering time gene CONSTANS. *Plant Cell* **12**, 2473-2484.

- **Yu, Y., Li, Y., Huang, G., Meng, Z., Zhang, D., Wei, J., Yan, K., Zheng, C. and Zhang, L.** (2011) PwHAP5, a CCAAT-binding transcription factor, interacts with PwFKBP12 and plays a role in pollen tube growth orientation in *Picea wilsonii*. *J. Exp. Bot.* **62**, 4805-4817.

Tables

Table 1. CONSTANS protein interactors in the Split-Ubiquitin System.

Gene identifier	Protein name	Protein description
At3g52360	-	Endomembrane protein involved in karrikin response
At2g20420	ATP citrate lyase (ACL)	Succinate-CoA ligase (GDP-forming) activity
At1g02290	NFRKB-RELATED	Related to kappa-B binding protein, INO80 complex
At2g40430	SMO4	Regulator of cell division in organ growth
At2g44065	Ribosomal protein	Structural constituent of ribosome
At3g27350	-	Nuclear protein of unknown function
At5g05370	Cytochrome b-c1 complex, subunit 8	Respiratory chain component
At4g31985	RPL39C	Structural constituent of ribosome
At2g42190	-	rho GTPase-activating gacO-like protein
At4g29390	RPS30D	Structural constituent of ribosome
At1g71695	PPXR6	Peroxidase protein; response to oxidative stress
At3g52500	Aspartyl protease	Aspartic-type endopeptidase activity
At5g17960	C1-clan protein	Hormone stress response
At3g21160	MNS2	N-glycan processing, root development
At1g58080	HISN1A	ATP phosphoribosyltransferase, Histidine biosynthetic process
At3g60640	ATG8G	Autophagy, cellular response to nitrogen starvation, protein transport, nuclear
At3g09840	CDC48A	Cell division cycle protein, member of AAA-type ATPase family
At3g28180	CSLC4	Cellulose synthase, cell wall organization
At1g29930	LHCB1.3	LHCII complex subunit, photosynthesis, response to light stimuli
At5g64350	FKBP12	Chaperone-mediated protein folding, peptidyl-proline modification, protein peptidyl-prolyl isomerization
At2g47180	GOLS1	Galactinol synthase, formation of galactinol from UDP-galactose and myo-inositol, Hexosyltransferase
At3g26650	GAPDHA1	Photosynthetic glyceraldehyde-3-phosphate dehydrogenase
At1g21130	IGMT4	Methyltransferase activity, protein dimerization activity
At3g57300	INO80	Member of the SWI/SNF ATPase family, chromatin remodelling
At2g38530	LTP2	Involved in lipid transfer between membranes, cell growth
At5g02380	MT2B	Metallothionein, cysteine-rich protein with copper-binding activity
At3g20970	ATNFU2	Contains NUF domain, iron-sulfur cluster assembly
At3g61990	OMTF3	Methyltransferase involved in the methylation of plant transmembrane proteins
At5g42790	PAF1	Extensive homology to the largest subunit of the multicatalytic proteinase complex (proteasome)
At3g25800	PP2A-A2	One of three protein phosphatase 2A regulatory subunit
At5g41700	UBC8	Constituent of the ubiquitin-conjugating enzyme E2

Figure legends

Figure 1. Interaction between CO and FKBP12. (a) Co-elution of S-tagged CO (S·CO) with His-tagged FKBP12 (H·FK) in *E. coli*. Immunoblots showing S·CO (above) and H·FK (below) presence in soluble extract (Introduction, In), binding to S·beads (Flow through, Ft), washing with buffer (W) and elution (El). αCO (above) and αHis-tag (below) antibodies were used. (b) Control experiment in which S·CO is expressed alone. (c) Confocal images of *Nicotiana* leafs co-infiltrated with 35S:*FKBP2:CFP* tag (FK-CFP, cyan) and 35S:*YFP:CO* (YFP-CO, yellow) constructs. FRET was measured by the acceptor photobleaching technique. White bar indicates 10 μm. The quantified efficiency of the interaction and negative control is shown on the right. (d) Immunoblot showing FKBP12 in total soluble fractions of Col-0, 35S:*CO* and *co-10* plants 15 DAG LD (left). 70 μg protein were loaded per lane and probed with αFK (Above) or antibody against cytosolic non-phosphorylating GAPDHN (αGAPN, below) as loading control. FKBP12 signal was quantified compared to control in three independent experiments and plotted (right). (e) Immunoblot showing CO levels in nuclear fractions of 35S:*CO,* Col-0 and *35S:FK* plants 15 DAG LD. 100 μg of protein from nuclear lysates were probed with αCO (above) and αHistone3 (αH3, below). CO signal was quantified compared to control in three independent experiments and plotted (right).

Figure 2. Molecular characterization of *FKBP12* expression. (a) 24 h qRT-PCR analysis of *FKBP12* expression in Col-0 (grey) and *fk12-1* mutant (black) under LD (left) and SD (right). *UBQ* was used as control. Error bars indicate s.d. from three independent experiments. (b) 24 h FKBP12 presence in total protein fractions of Col-0, *35S:FK* and *fk12-1* plants 15 DAG LD (left) and quantification of protein levels in three replicates by Western blot using αFK (right). 40 μg protein were loaded per lane. (c) 24 h immunoblot analysis of CO (CO, above, left) and FKBP12 (FK, below, left) using αCO and αFK in total protein fractions from 35S:*CO* plants 15 DAG LD. Graphic (right) represents CO and FKBP12 levels from three protein extracts compared to control. 40 μg of protein were loaded per lane. (d) 24 h qRT-PCR analysis of *CO* expression (above) and *FT* expression

(below) in Col-0, *fk12-1* and 35S:*FK* in 15 DAG LD plants. *UBQ* gene was used as control. Error bars indicate s.d. from three independent experiments.

Figure 3. Flowering signals associated with FKBP12 levels. (a) Immunoblot showing CO and FKBP12 levels in nuclear fractions of Col-0, 35S:*FK* and *fk12-5* plants 15 DAG (ZT16) LD (above). 100 μg of protein from nuclear lysates were probed with αCO, αFK and αH3. CO signal was quantified as phosphorylated (upper form) and non-phosphorylated (lower form), compared to control in three independent experiments and plotted (below, left). Ratio of phosphorylated (upper form) and non-phosphorylated (lower form) was quantified and compared to control in three independent experiments and plotted (below, right). (b) Immunoblot showing FT in total soluble fractions of Col-0, *fk12-1* and 35S:*FK* plants 15 DAG (ZT4) LD (left). 70 μg protein were loaded per lane and probed with αFT. FT signal was quantified compared to control in three independent experiments and plotted (right). (c) Comparison of flowering time (above) and rosette and cauline leaves (middle) in Col-0, 35S:*FK, fk12-1* and *fk12-5* plants under LD conditions. Graphic bar showing flowering time of Col-0, 35S:*FK*, *fk12-1* and *fk12-5* plants in LD (below). Black bars, rosette leaves; grey bars, cauline leaves. Error bars indicate s.d. of at least 50 plants. Asterisks indicate statistically significant differences with Col-0: * $P<0.05$, ** $P<0.01$, *** $P<0.001$.

Figure 4. CO is stabilized by FKBP12. (a) immunoblot (left) and quantification of CO levels (right) expressed alone (H·CO) and co-expressed with FKBP12 (H·CO S·FK) in bacteria. 30 μg protein were loaded per lane and probed with αCO and αFK. Nonspecific bands were used as loading controls (CONT). Right, bar graphs representing the means of protein amounts (± s.d.) from at least three independent experiments. (b) immunoblot using αCO and αFK showing column elution of H·CO (left pannels) and H·CO S·FK (middle panels) extracts after rapamycin (Rap) and FK506 treatments. Nonspecific bands were used as loading controls (CONT). Right, bar graphic showing CO amount quantification in the experiments left, representing the means (± s.d.) of at least three independent experiments. (c) Y2H analysis of the interaction between FKBP12 (FK) and different domains of CO (BBOX, MIDdle and CCT). Left, interactions are shown by blue dye (X-Gal,

lower panel) and growth on selective media (-Leu, middle panel). Growth on normal media is also shown (CONT, upper panel). Yeast transformed with empty plasmid pEG202:pJG4-5 (-) was used as negative control. Pictures show 3-day-old colonies. Right, quantification of B-Gal activity (B-gal units x 10^4). (d) Confocal images of BiFC analysis in *Nicotiana* epithelial cells showing protein-protein interactions between different domains of CO (BBOX, MIDdle and CCT). The white bars represent 26 μm. Asterisks indicate statistically significant differences: ** P<0.01, *** P<0.001.

Figure 5. FKBP12-CO interaction is destabilized by CO mutation in VP pairs. (a) immunoblot analysis (above) and bar graphic showing the quantification (below) of H·CO and H·CO* levels co-expressed with S·FK in bacterial soluble fractions and total cell crude lysates. 30 μg of protein were probed with αCO and αFK. Extracts from bacteria carrying empty plasmids were used as negative controls (-). Nonspecific bands were used as loading control (CONT). Bar graphics represent the means (± s.d.) of at least three independent experiments. White bars: CO amount (R.U.). Grey bars: FKBP12 amount (R.U.). (b) Confocal images of BiFC analysis in *Nicotiana* epithelial cells showing protein-protein interactions between NYFP:CO and CYFP:FK (above) and NYFP:CO* and CYFP:FK (below). The white bars represent 10 μm.

Figure 6. FKBP12 is conserved in the photosynthetic linage. (a) Subcellular localization of *Chlamydomonas* FKBP12 (CrFKBP12). Confocal images of CW15 cells expressing *CrFKBP12:YFP* (below) and CW15 cells transformed with empty plasmid (Above) as negative control. SYTO Blue 45 staining was used as nuclear marker. Bar represents 10 μm. (b) Confocal images of BiFC analysis in *N. benthamiana* epithelial cells showing protein-protein interactions between NYFP:CrCO-CYFP:CrFKBP12 (left), NYFP:AtCO-CYFP:CrFKBP12 (middle) and NYFP:CrCO-CYFP:AtFKBP12 (right). Bar represents 26 μm (left and middle) and 14 μm (right).

Figure 7. Molecular mechanism for CO-FKBP12 interaction. FKBP12 interacts with CO and stabilizes the phosphorylated form in the nucleus, promoting *FT* expression and the

flowering signal (black arrows). The model suggests that FKBP12-CO interaction stabilizes the phosphorylated form by preventing CO-COP1 interaction and the following CO degradation by the proteasome (grey arrows).

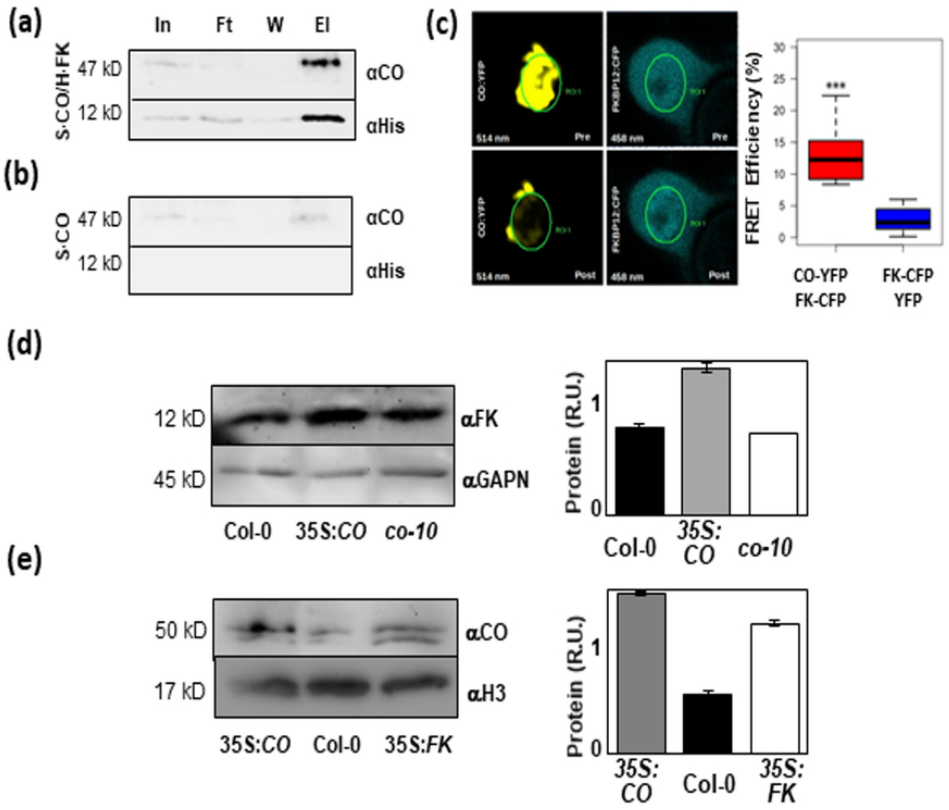

FIGURE 1

77x68mm (300 x 300 DPI)

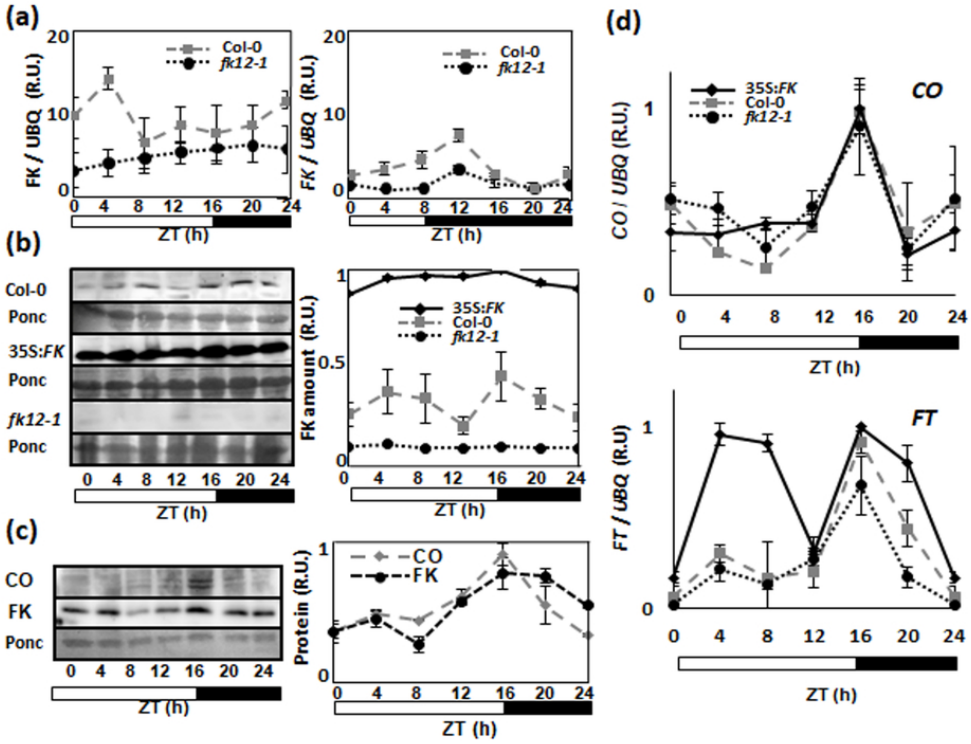

FIGURE 2

80x61mm (300 x 300 DPI)

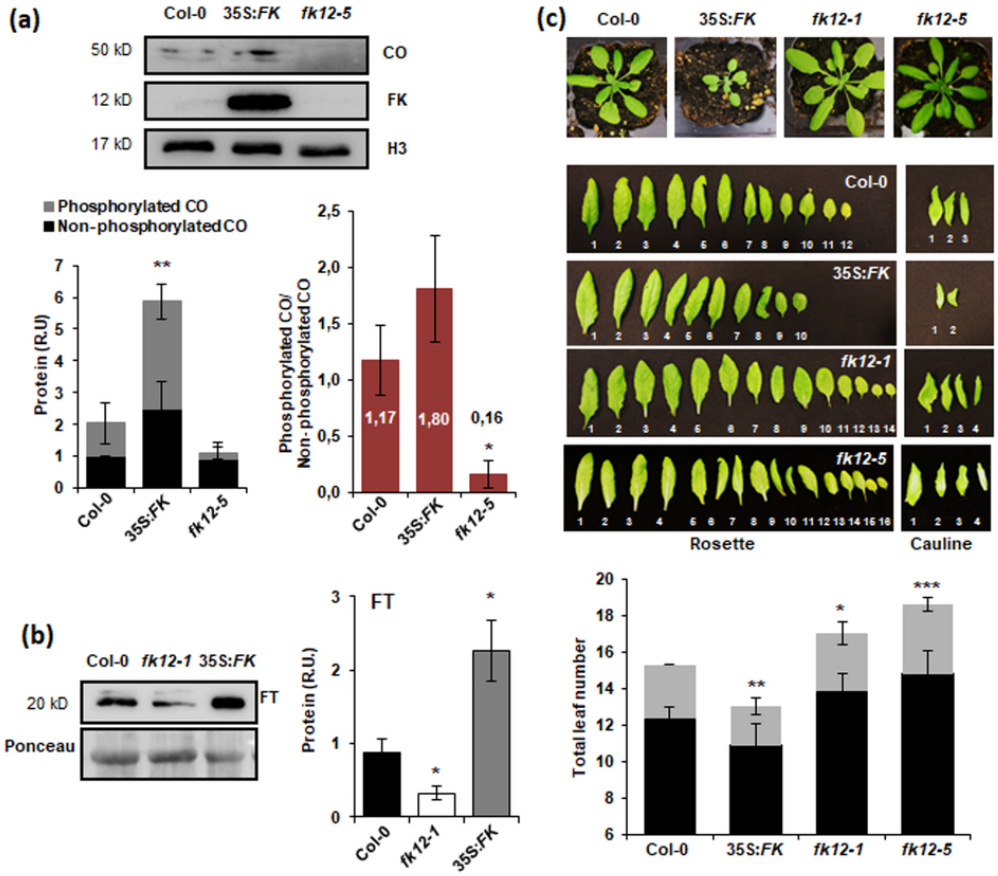

FIGURE 3

80x72mm (300 x 300 DPI)

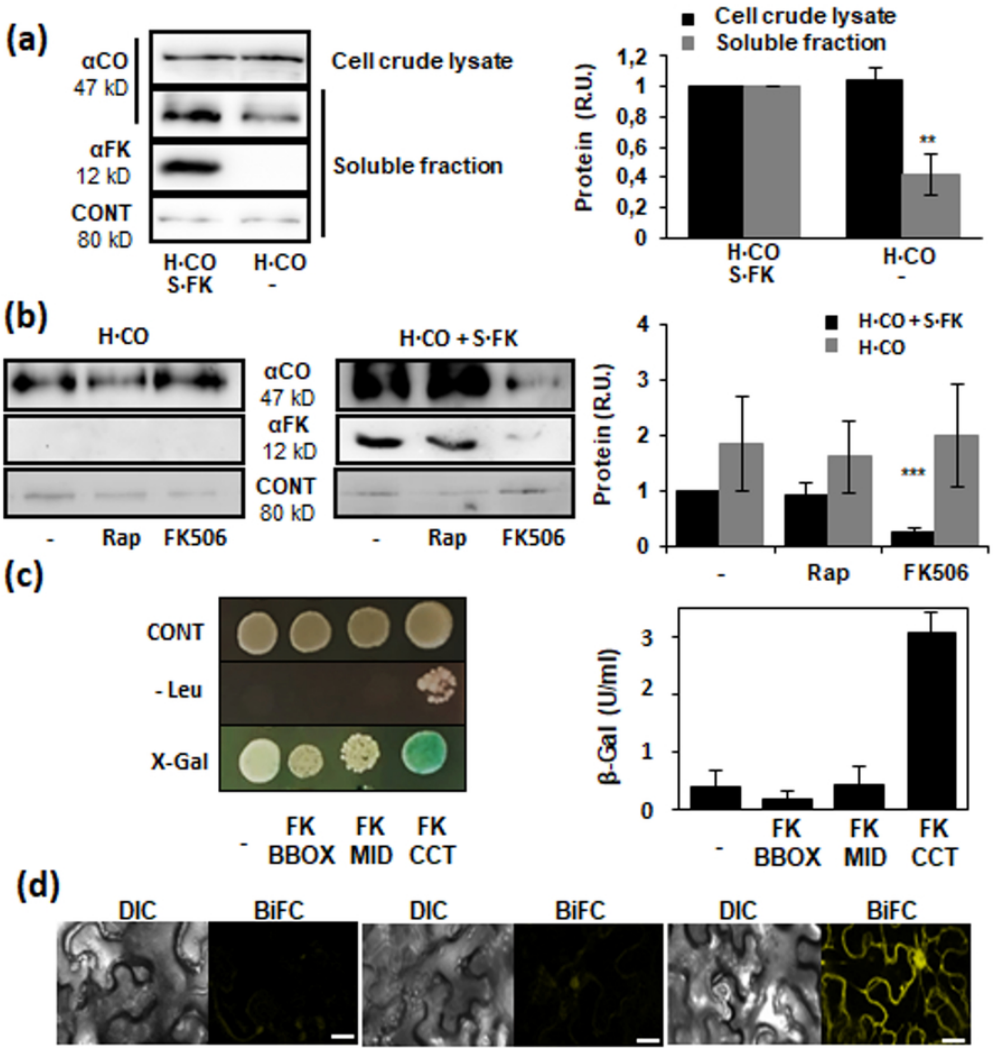

FIGURE 4

75x80mm (300 x 300 DPI)

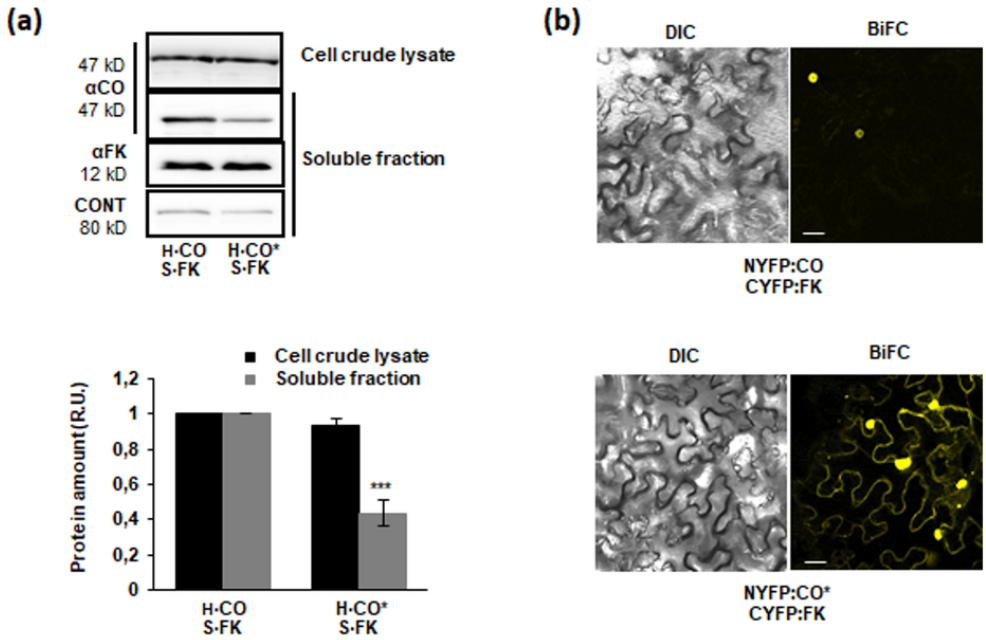

FIGURE 5

80x52mm (300 x 300 DPI)

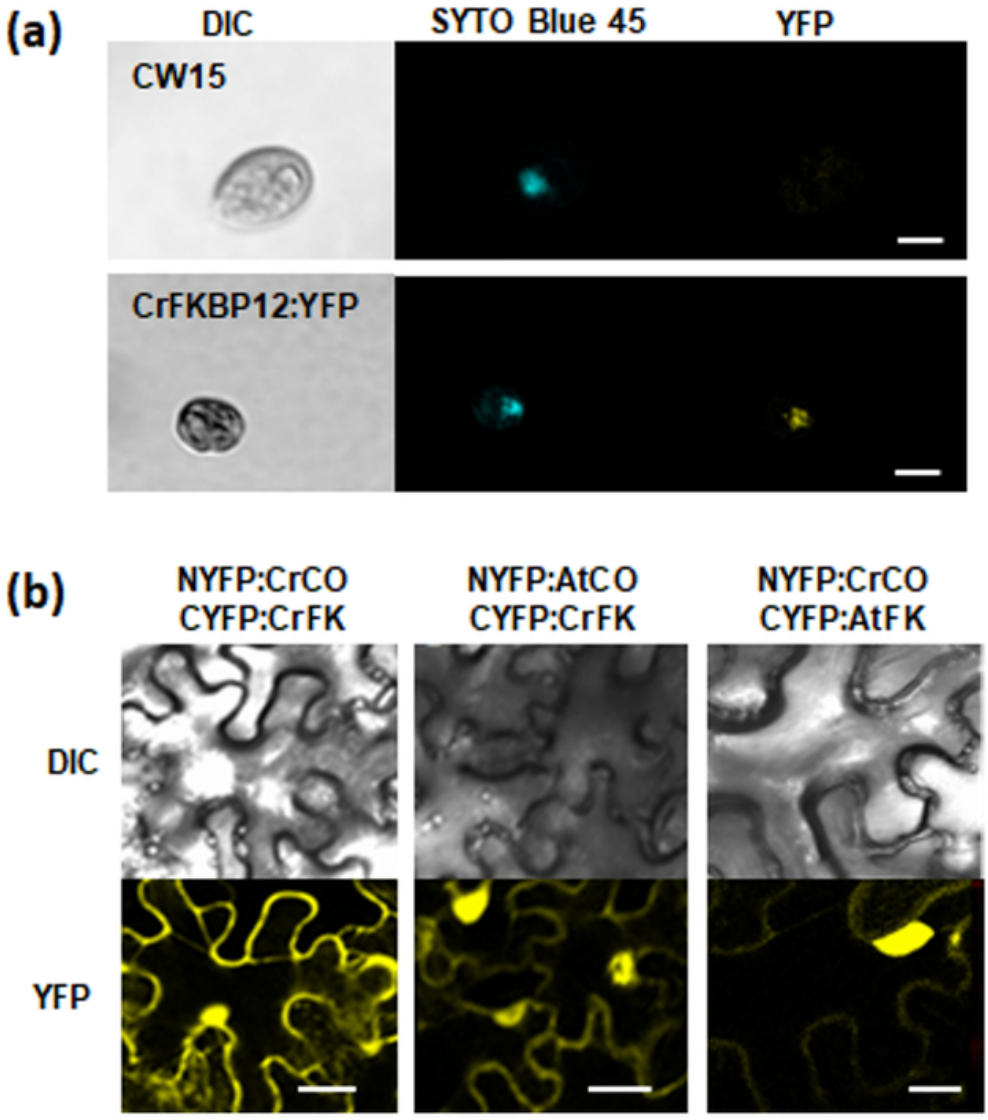

FIGURE 6

53x59mm (300 x 300 DPI)

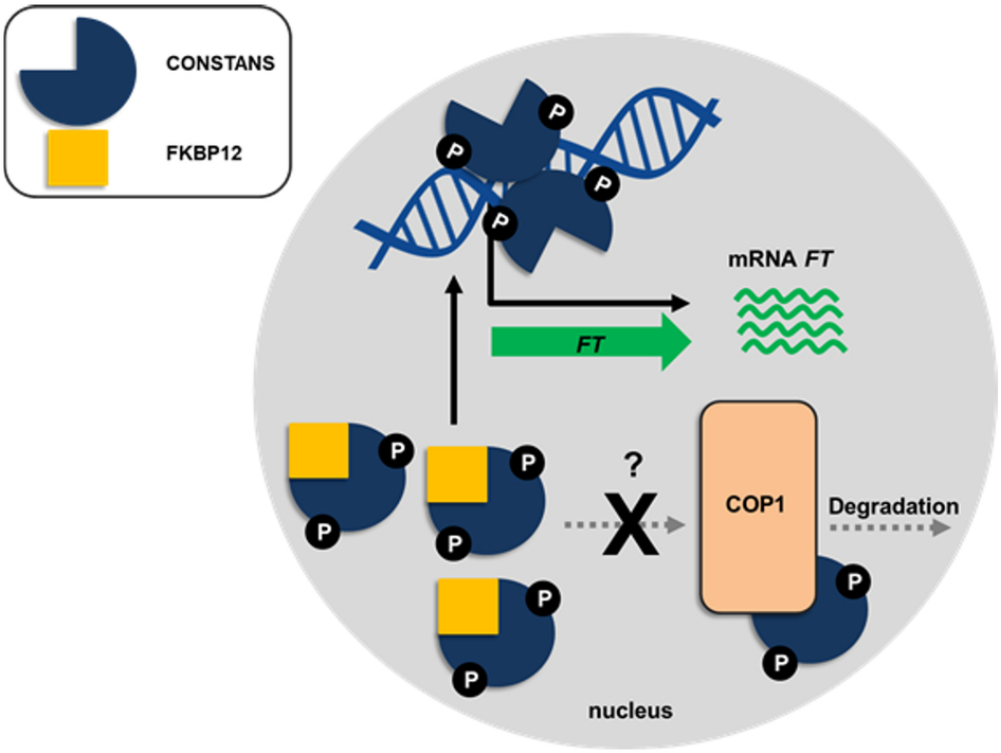

FIGURE 7

80x60mm (300 x 300 DPI)

SIGNIFICANCE STATEMENT

Posttranscriptional regulation of CONSTANS (CO) protein is essential to promote photoperiodic flowering in *Arabidopsis thaliana*, and here we show that the interaction with the immunophilin FKBP12 promotes CO stabilization and activity, so that *fkbp12* mutants are late flowering, while overexpression promotes early flowering. The conserved interaction between algal and plant CrCO-CrFKBP12 orthologues reflects the evolutionary importance of this interaction.

Figure S1

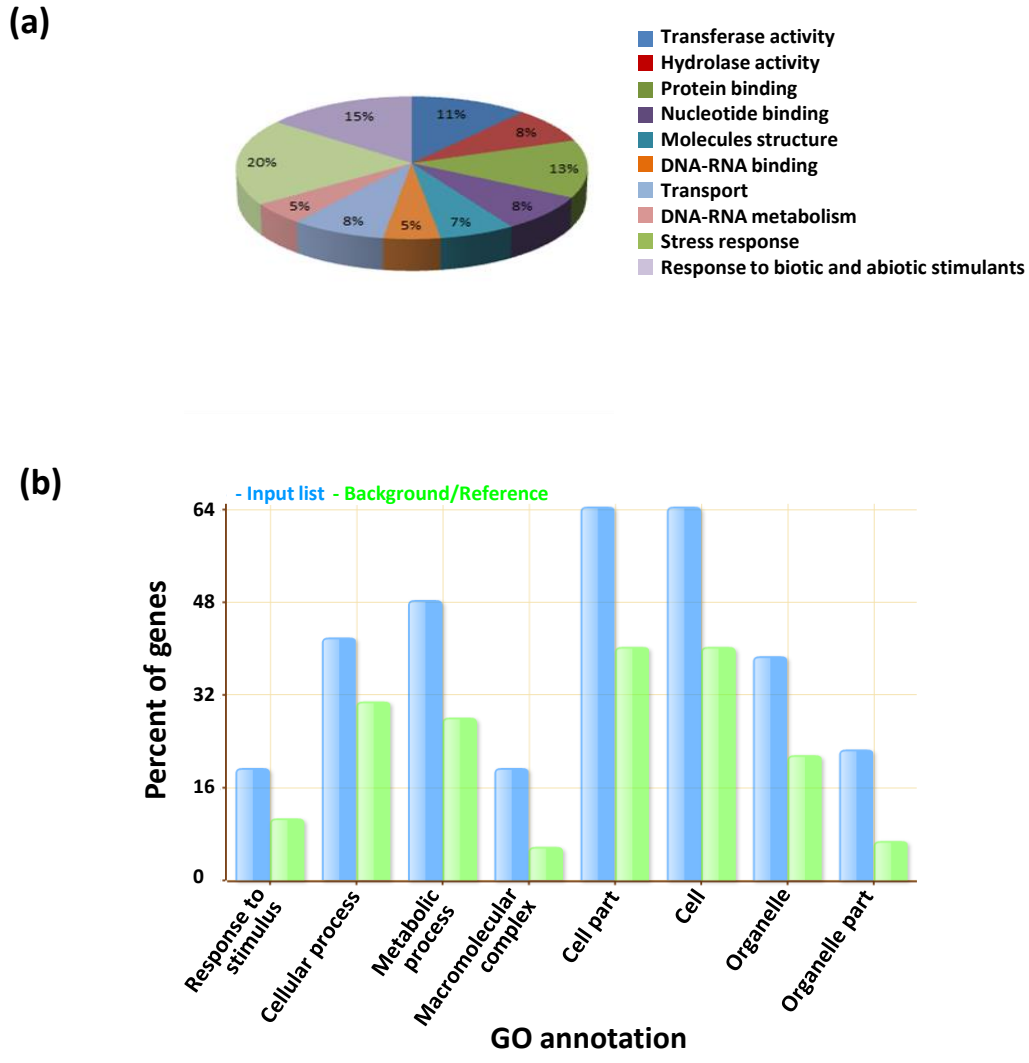
(a)
11%
8%
13%
8%
7%
5%
8%
5%
20%
15%
Transferase activity
Hydrolase activity
Protein binding
Nucleotide binding
Molecules structure
DNA-RNA binding
Transport
DNA-RNA metabolism
Stress response
Response to biotic and abiotic stimulants
(b)
- Input list - Background/Reference
Percent of genes
64
48
32
16
0
Response to stimulus
Cellular process
Metabolic process
Macromolecular complex
Cell part
Cell
Organelle
Organelle part
GO annotation

Figure S2

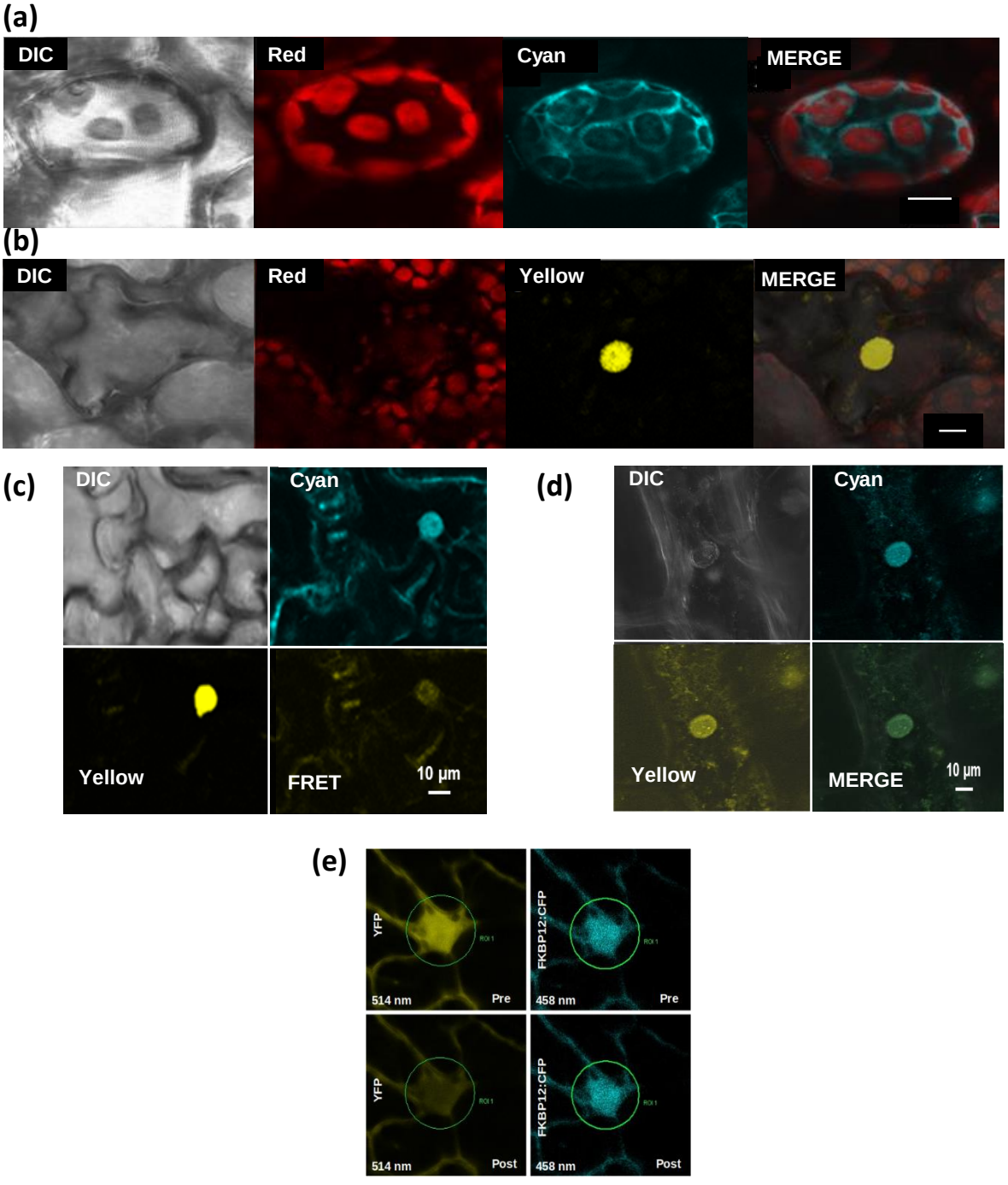
(a)
DIC
Red
Cyan
MERGE
(b)
DIC
Red
Yellow
MERGE
(c)
DIC
Cyan
Yellow
FRET
10 µm
(d)
DIC
Cyan
Yellow
MERGE
10 µm
(e)
YFP
514 nm
Pre
FKBP12:CFP
458 nm
Pre
YFP
514 nm
Post
FKBP12:CFP
458 nm
Post

Figure S3

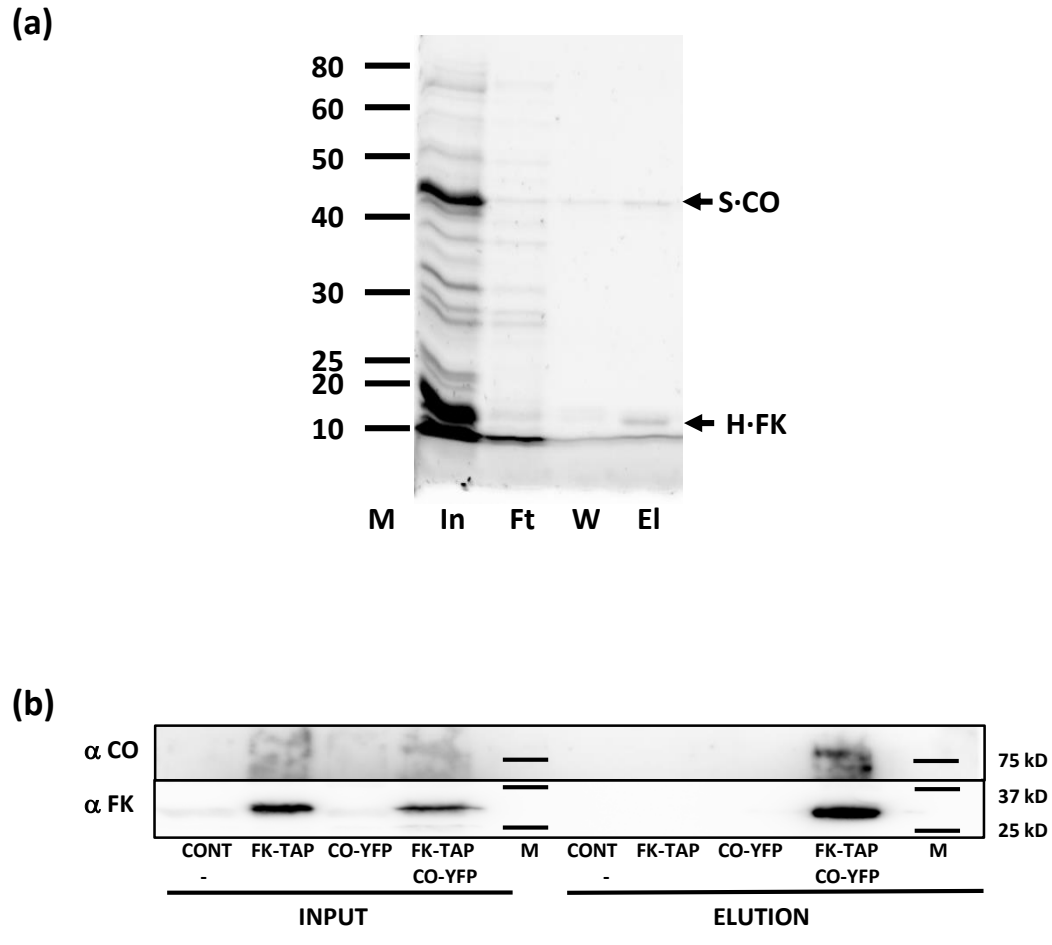
(a)
80
60
50
40
30
25
20
10
S·CO
H·FK
M
In
Ft
W
El
(b)
α CO
α FK
75 kD
37 kD
25 kD
CONT
-
FK-TAP
CO-YFP
FK-TAP
CO-YFP
M
CONT
-
FK-TAP
CO-YFP
FK-TAP
CO-YFP
M
INPUT
ELUTION

Figure S4

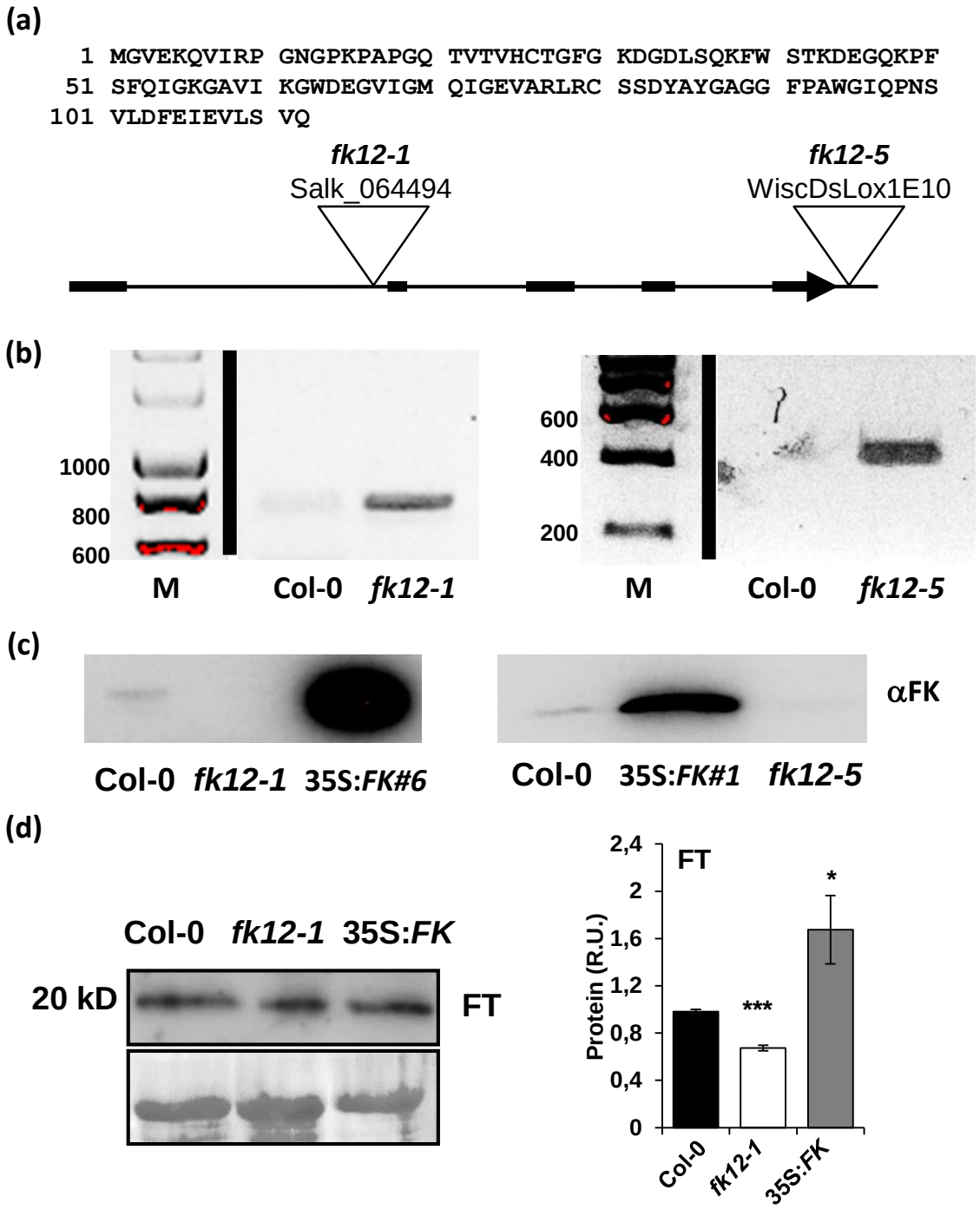
(a)
1 MGVEKQVIRP GNGPKPAPGQ TVTVHCTGFG KDGDLSQKFW STKDEGQKPF
51 SFQIGKGAVI KGWDEGVIGM QIGEVARLRC SSDYAYGAGG FPAWGIQPNS
101 VLDFEIEVLS VQ
fk12-1
Salk_064494
fk12-5
WiscDsLox1E10
(b)
1000
800
600
M
Col-0
fk12-1
600
400
200
M
Col-0
fk12-5
(c)
Col-0
fk12-1
35S:FK#6
Col-0
35S:FK#1
fk12-5
αFK
(d)
Col-0
fk12-1
35S:FK
20 kD
FT
FT
Protein (R.U.)
2,4
2
1,6
1,2
0,8
0,4
0
***
*
Col-0
fk12-1
35S:FK

Figure S5

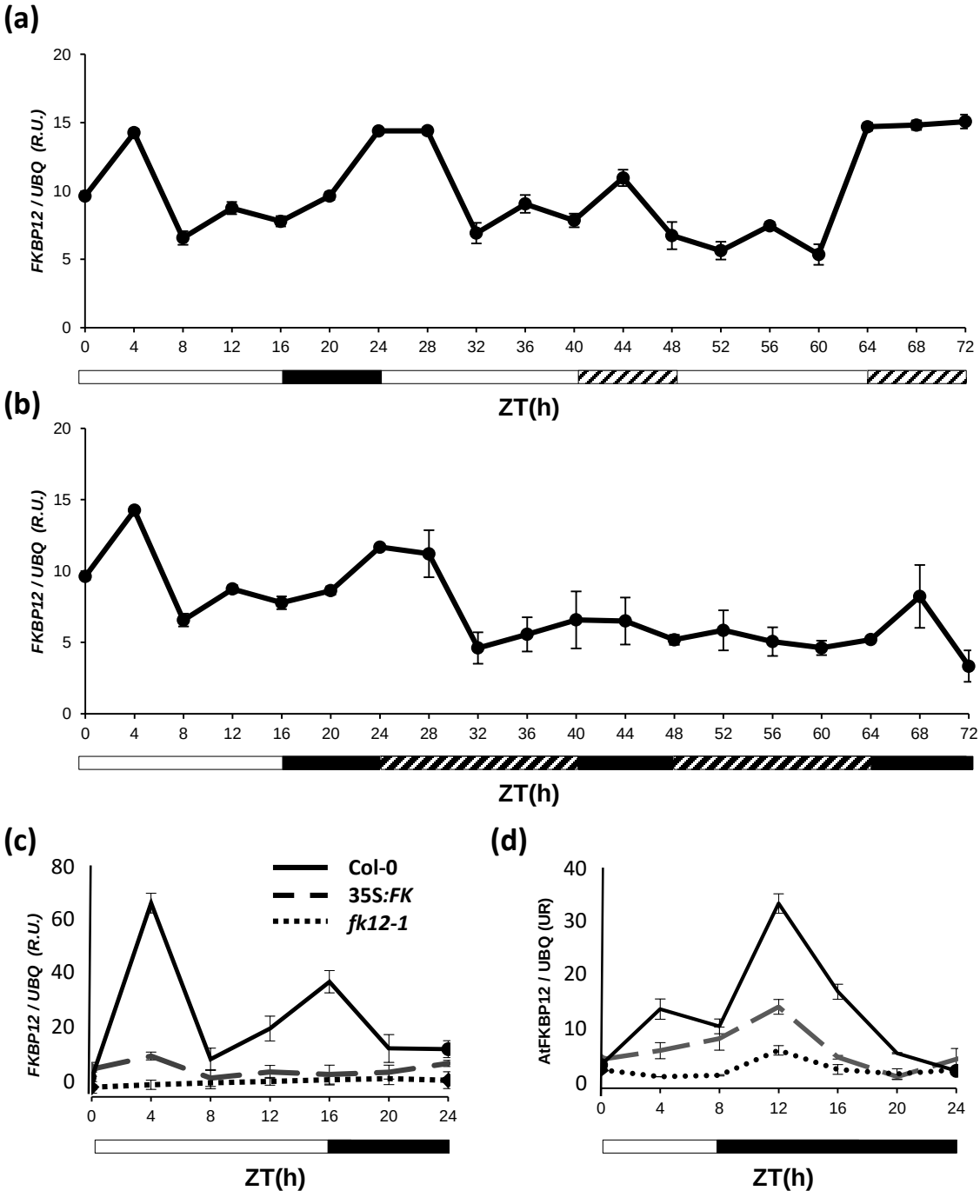
(a)
FKBP12 / UBQ (R.U.)
ZT(h)
(b)
FKBP12 / UBQ (R.U.)
ZT(h)
(c)
Col-0
35S:FK
fk12-1
FKBP12 / UBQ (R.U.)
ZT(h)
(d)
AtFKBP12 / UBQ (UR)
ZT(h)

Figure S6

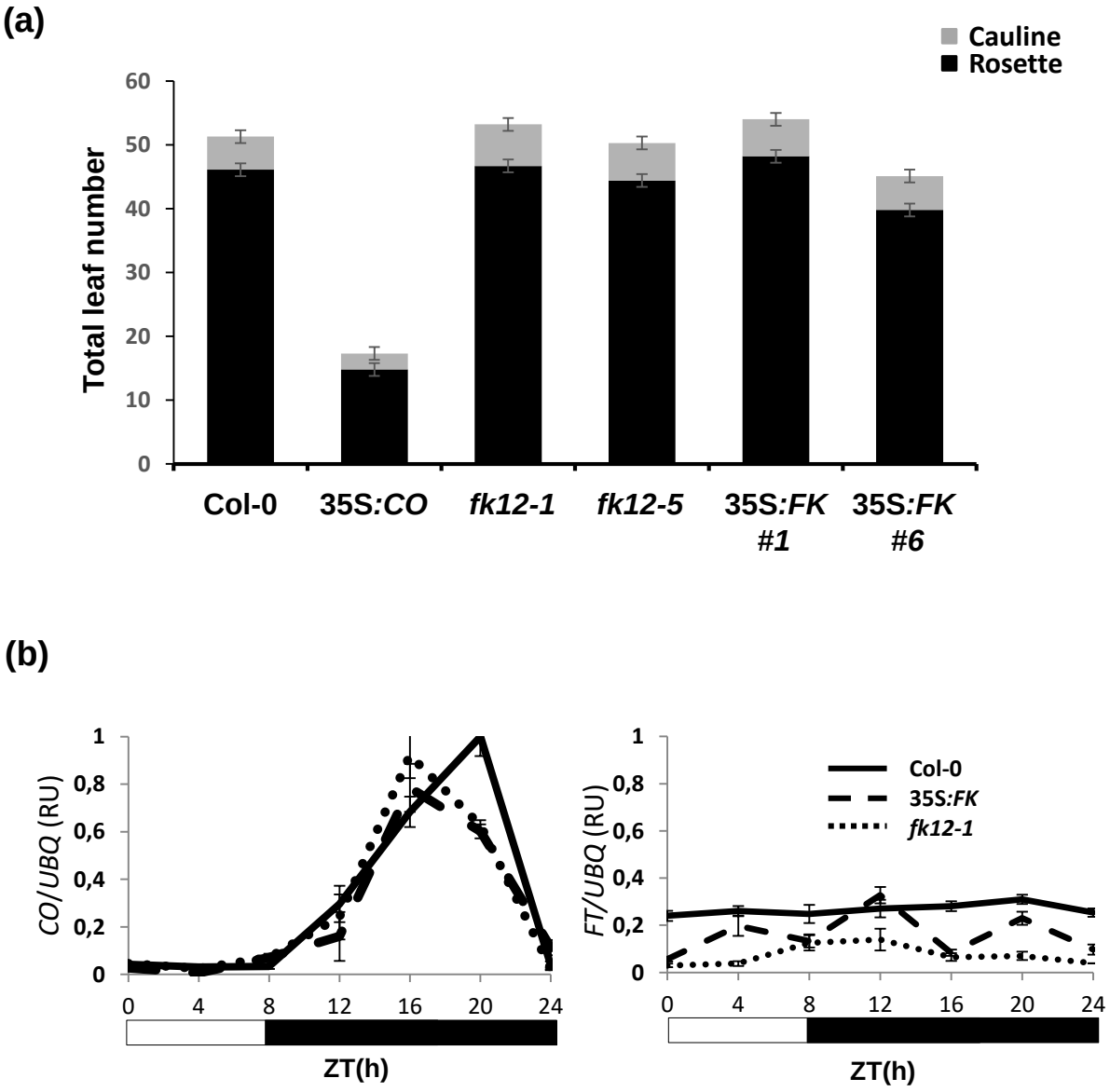
(a)
Cauline
Rosette
Total leaf number
60
50
40
30
20
10
0
Col-0
35S:CO
fk12-1
fk12-5
35S:FK #1
35S:FK #6
(b)
CO/UBQ (RU)
1
0,8
0,6
0,4
0,2
0
0 4 8 12 16 20 24
ZT(h)
FT/UBQ (RU)
Col-0
35S:FK
fk12-1
ZT(h)

Figure S7

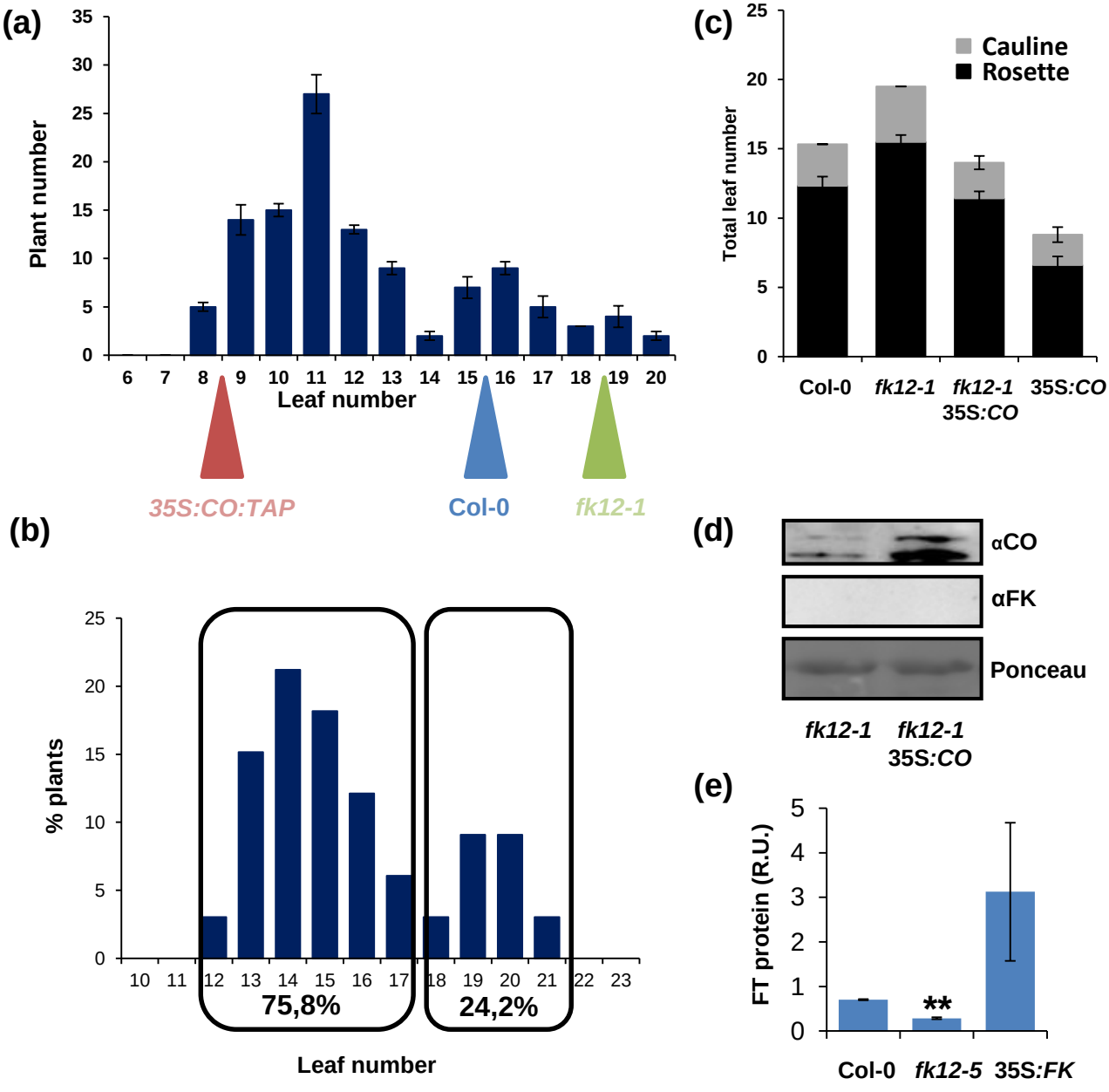
(a)
Plant number
Leaf number
35S:CO:TAP
Col-0
fk12-1
(b)
% plants
75,8%
24,2%
Leaf number
(c)
Cauline
Rosette
Total leaf number
Col-0
fk12-1
fk12-1 35S:CO
35S:CO
(d)
αCO
αFK
Ponceau
fk12-1
fk12-1 35S:CO
(e)
FT protein (R.U.)
**
Col-0
fk12-5
35S:FK

Figure S8

(a)

```
  1 MLKQESNDIG SGENNRARPC DTCRSNACTV YCHADSAYLC MSCDAQVHSA
 51 NRVASRHKRV RVCESCERAP AAFLCEADDA SLCTACDSEV HSANPLARRH
101 QRVPILPISG NSFSSMTTTH HQSEKTMTDP EKRLVVDQEE GEEGDKDAKE
151 VASWLFPNSD KNNNNQNNGL LFSDEYLNLV DYNSSMDYKF TGEYSQHQQN
201 CSVPQTSYGG DRVVPLKLEE SRGHQCHNQQ NFQFNIKYGS SGTHYNDNGS
251 INHNAYISSM ETGVVPESTA CVTTASHPRT PKGTVEQQPD PASQMITVTQ
301 LSPMDREARV LRYREKRKTR KFEKTIRYAS RKAYAEIRPR VNGRFAKREI
351 EAEEQGFNTM LMYNTGYGIV PSF
```

(b)

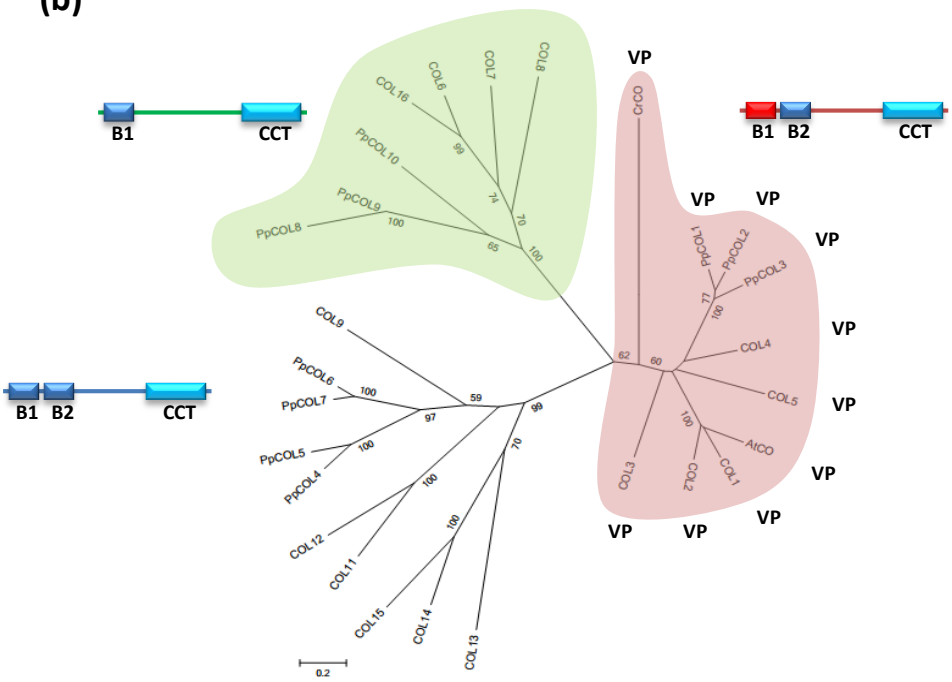

(c)

Protein	Gene identifier
CrCO	g6302
PpCOL1	Pp1s371_27V6
PpCOL2	Pp1s97_109V6
PpCOL3	Pp1s364_5V6
PpCOL4	Pp1s36_238V6
PpCOL5	Pp1s26_5V6
PpCOL6	Pp1s236_21V6
PpCOL7	Pp1s195_82V6
PpCOL8	Pp1s143_52V6
PpCOL9	Pp1s108_97V6
PpCOL10	Pp1s3_491V6
CO	At5g15840
AtCOL1	At5g15850
AtCOL2	At3g02380
AtCOL4	At5g24930
AtCOL5	At5g57660
AtCOL6	At1g68520
AtCOL7	At1g73870
AtCOL8	At1g49130
AtCOL9	At3g07650
AtCOL1O	At5g48250
AtCOL11	At4g15250
AtCOL12	At3g21880
AtCOL13	At2g47890
AtCOL14	At2g33500
AtCOL15	At1g28050
AtCOL16	At1g25440

Figure S9

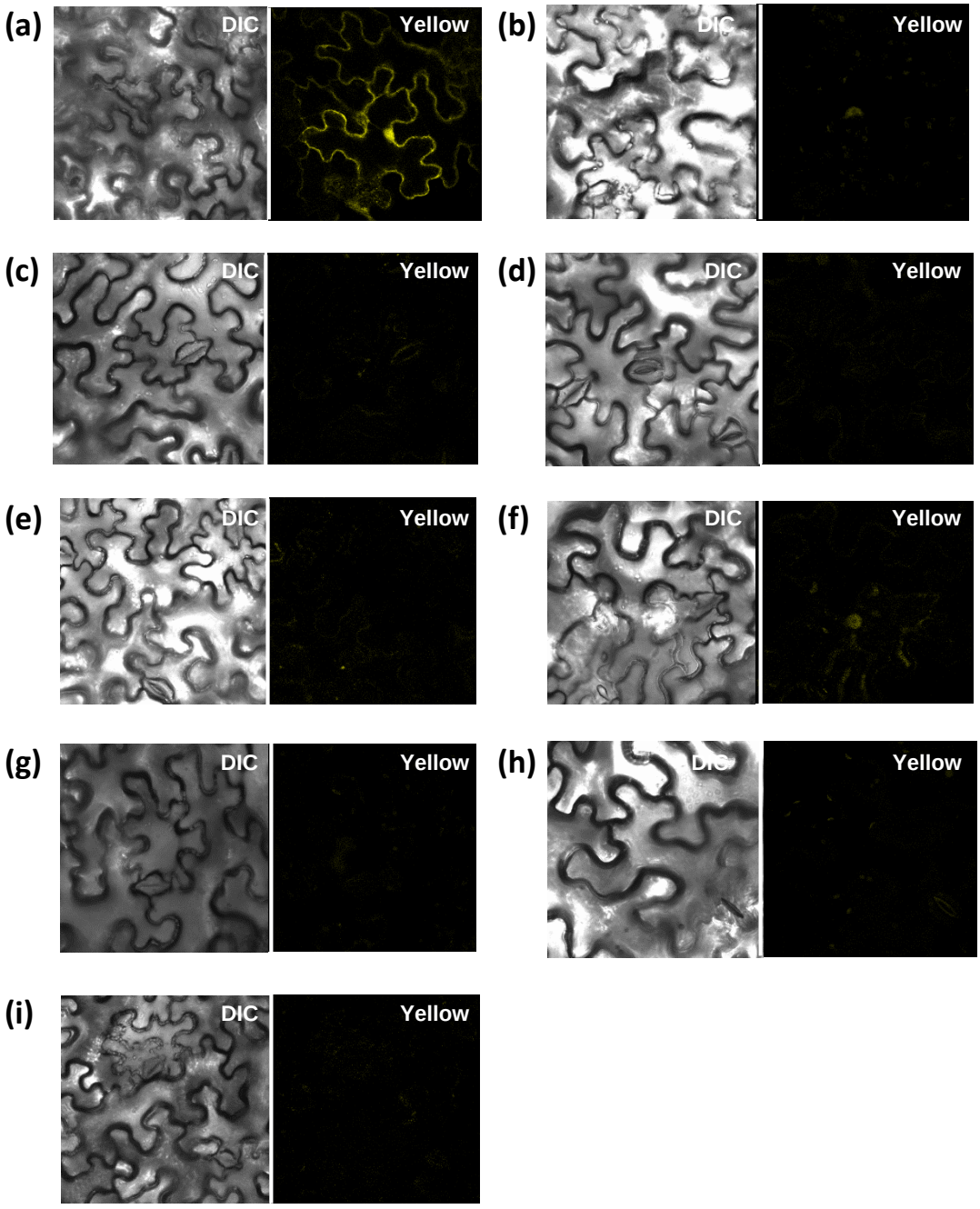
(a)
DIC
Yellow
(b)
DIC
Yellow
(c)
DIC
Yellow
(d)
DIC
Yellow
(e)
DIC
Yellow
(f)
DIC
Yellow
(g)
DIC
Yellow
(h)
DIC
Yellow
(i)
DIC
Yellow

Figure S10

(a)